The Excited State Absorption Cross Section of Neodymium-doped Silica Glass Fiber in the 1200-1500 nm Wavelength Range

By
Nicholas H. P. Verlinden

A Thesis
Submitted to the Faculty
of the
WORCESTER POLYTECHNIC INSTITUTE
in partial fulfillment of the requirements for the
Degree of Master of Science
in
Physics
July 2008

APPROVED:

_____

Professor Richard S. Quimby, WPI – Major Thesis Advisor

_____

Professor Rafael Garcia, WPI

Abstract

Hydroxyl ions are a common contaminant in optical fibers, and are responsible for strong absorption centered at 1380 nm that becomes significant over long optical path lengths. Recently, however, special fabrication methods have been developed that minimize the hydroxyl ion contamination, permitting use of the entire 1300-1700 nm spectral region for telecommunications. There is therefore interest in examining the Nd $^4F_{3/2}$ to $^4I_{13/2}$ transition for a potential optical amplifier at 1400 nm. In this thesis, the excited state absorption cross section and the overall gain/loss spectrum of neodymium in a silica glass fiber were determined for the 1200-1500 nm wavelength region using the pump-probe method. The ground state absorption cross section was also determined from transmission measurements, and the stimulated emission cross section was calculated using the fluorescence spectrum and the McCumber relation. Oscillator strengths for absorption and emission transitions were calculated in the 800-1600 nm wavelength range using the Judd-Ofelt method. The above procedures were followed for both the Nd-doped fiber, as well as an erbium-doped silica fiber. The shape of the Nd emission spectrum is also noteworthy, since the characteristic Nd peak at 1064 nm is not observed, although there is strong emission at 1092 nm. The pump-probe measurements revealed significant excited state absorption loss between 1200 and 1350 nm, due to excitation from the $^4F_{3/2}$ to the higher $^4G_{9/2}$ and $^4G_{7/2}$ states. Between 1350 and 1475 nm, there was no net gain or loss that could be observed beyond the level of the noise. For the glass fibers studied, it appears that in the spectral region of interest for an optical amplifier, the stimulated emission and excited state absorption cancel one another out.

Acknowledgements

There are countless individuals who have helped or inspired me during my studies, but I would like to recognize those who had the greatest impact on the successful completion of my thesis and degree.

Professor Richard Quimby was my project advisor for both this work and my MQP. His patience and guidance made him a pleasure to work for. I am continually impressed by his depth of knowledge and his help was very much appreciated.

My academic advisor, Professor Carolann Koleci was always helpful and supportive throughout my entire WPI career. She was one of my first teachers, and I learned much both as her student and as a TA for her courses.

I would like to extend a special thank-you to my family. My parents have always been there for me, even from across the country, and I could not ask for a better brother. Without their love and support, this accomplishment would have been impossible.

Additionally, I would like to thank the physics department and the graduate committee for the opportunity to continue my education here at WPI. In particular, Professors Nancy Burnham and P.K. Aravind were very helpful and have always been forthcoming with advice and guidance. I am also grateful to Professor Rafael Garcia for his participation in the review and completion of this thesis.

Finally, I wish to acknowledge Roman Shubochkin from Boston University as the provider of the sample fibers used in this study.

Table of Contents

Table of Figures

Table of Tables

1. Introduction

The absorption of light at 1380 nm by hydroxyl ions (OH^-) has prohibited the use of that wavelength window for optical communications. These OH^- ions are a common contaminant, due in large part to the humidity in the air. The absorption is not strong when compared to rare-earth ion transitions; however, over the distances used for communications it is sufficient to render the wavelength unusable. For this reason, neodymium-doped fibers have not been used as amplifiers in this wavelength region despite the fact that neodymium (Nd) has an emission transition peak at approximately 1340 nm. As it becomes possible to create optical fibers with minimal hydroxyl ion contamination, there is renewed interest in Nd-doped fibers for use as amplifiers.

Optical amplifiers are based upon the same principle as lasers: stimulated emission. Energy is added to the amplifier medium (called pumping), often optically through the use of a laser, and the neodymium (or other rare-earth) ions are excited. Rare-earth elements have at least one excited state that has sufficient lifetime to sustain an excited population, provided there is a source of energy. The excited ion can relax to a lower energy state by emitting a photon with energy equal to the difference in energy between the states. It can either do this randomly, in any direction, or when it is struck by another photon that has the same energy. If this second process occurs, it is called stimulated emission, and the 'new' photon has the same characteristics as the incident photon and travels in the same direction. Each time this occurs, the amount of light from the original signal increases. It is also possible, however, for the excited ion to absorb a photon if there is an energy state above it with an energy difference equal to that of the incident photon.

As mentioned above, neodymium exhibits emission at approximately 1340 nm, but there can also be excited state absorption around 1300 nm. The relative magnitudes and spectral shapes of excited absorption and emission transitions will determine how much, if any, gain can be achieved in the region between 1200 and 1500 nm. The figure below is a measured gain loss spectrum of Nd doped into a Germanium-Silica glass fiber.

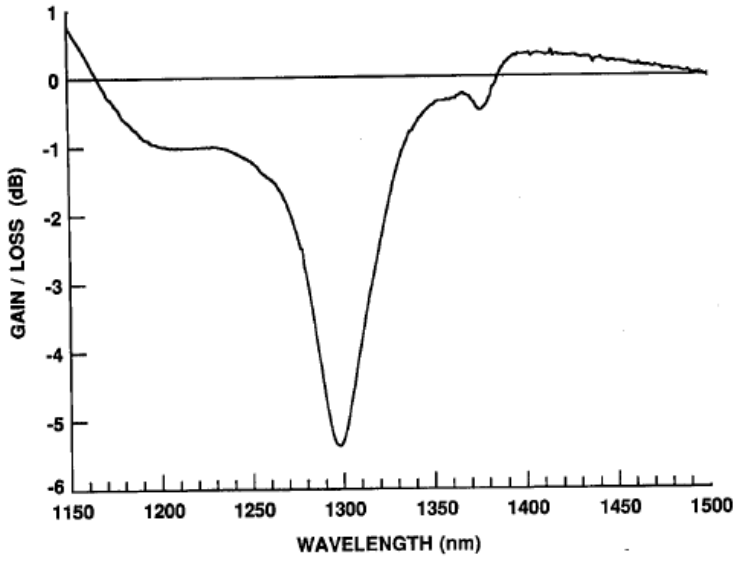

Figure 1: The gain/loss spectrum for Nd doped in a Ge-silica fiber [Miniscalco, 2001].

The effect of the 1300 nm excited state absorption on the overall gain/loss for Nd is displayed in Figure 1. At wavelengths between 1400 and 1450 nm, there is the possibility for gain, the demonstration of which will be attempted in this thesis. The excited state absorption cross section between 1200 and 1500 nm will also be determined.

The sample will be a 2-meter long neodymium-doped silica glass fiber. The pump-probe method will be used to measure the excited state absorption of the Nd-doped fiber. This method consists of coupling both a small tunable probe signal and a laser pump source into the doped fiber. Measurements are then taken of the transmission of the reference signal when the laser is switched on and off. The comparison of these measurements will yield a gain/loss spectrum like that seen above. Knowledge of the ground state absorption and stimulated emission cross sections are also required to determine the excited state absorption. The transmission of the light from a tungsten bulb through the fiber will be compared with the spectrum of the bulb to determine the ground state absorption cross section. The stimulated emission cross section will be obtained by measuring the fluorescence of the pumped fiber, out the side of the fiber, so there will be negligible re-absorption of the fluorescence. This fluorescence data will be converted to the stimulated emission cross section by using a combination of the McCumber relation and Judd-Ofelt theory.

2. Background Information

2.1 Energy Level Transitions

An electron in an atom can make a transition between discrete energy levels via three different optical processes: absorption, spontaneous emission, and stimulated emission.

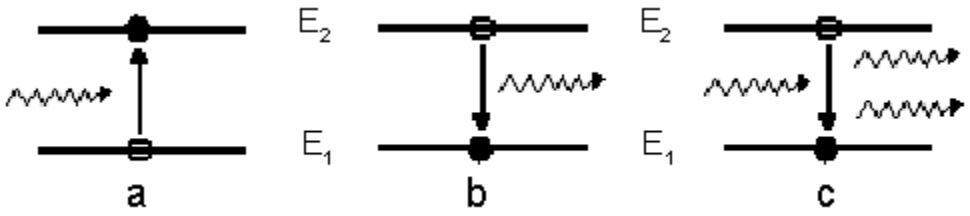

Figure 2: Illustrates absorption (a), spontaneous emission (b), and stimulated emission (c). E_1 and E_2 represent the energies of the two states.

Absorption, part *a* of the above figure, occurs when an incoming photon causes an electron to enter a higher energy state. The photon no longer exists, having 'given' all its energy to the particle. The probability for a single particle to absorb a single incident photon is dependent on the particle's absorption cross section, a quantity in units of area that varies with wavelength. The photon must have energy equivalent to the difference in energy levels, E_1 and E_2, for it to be absorbed. If the electron begins in its lowest energy state, this is referred to as 'ground state absorption'. If the electron is already in an excited state, and its energy level is raised further by an incoming photon, this is referred to as 'excited state absorption'. The following relation relates the energy of a photon to its frequency, ν, or wavelength, λ:

$$E_\gamma = h\upsilon = \frac{hc}{\lambda} \qquad (2.1\text{-}1)$$

Spontaneous emission occurs when an electron in an elevated energy state decays to a lower, unoccupied, level. The energy difference between the two levels is accounted for by the release of a photon with that energy. Multiple photons emitted by spontaneous emission between two energy levels will have the same frequency and wavelength because they have the same energy, but will have random phase and polarization. It is also possible for an electron to decay from an excited state via phonons, in which case no

light is emitted. In general, the smaller the energy gap between two levels, the more likely an electron would decay via phonons. Each excited state has an effective lifetime, after which 1/*e* of the electrons originally in that state will remain. Transitions with a higher probability of decaying via phonons generally have much shorter lifetimes.

An electron can also decay to a lower level through an interaction with a photon. If an excited electron is struck by a photon with energy equal to the difference in energy between the electron's current state and an unoccupied lower state, there is a probability the electron will decay to that state. If it does so, the excess energy is released in the form of a photon identical to the incident photon traveling in the same direction, with the same phase and polarization. This process is known as stimulated emission and is illustrated in part *c* of Figure 2. This probability, like that of absorption, is also governed by a cross section.

2.2 Neodymium Characteristics

Neodymium is a rare-earth element in the Lanthanide group. Rare-earth elements are commonly chosen as dopants for laser and amplification systems due to their narrow well-defined spectra and low non-radiative decay rates from certain energy levels. These elements have a partially full 4*f* electron band. These 4f electrons are the atom's valence electrons although they are not the furthest from the nucleus. Electrons in this state are partially shielded from what is known as the Crystal Field Effect, the change of an atom's Hamiltonian due to a host material, by the 5*s* and 5*p* electrons, which are further out from the nucleus. This means that rare-earth ion energy levels are not greatly affected by different host materials, and that optical transitions remain relatively narrow and well defined.

In neodymium, the ground state, $^4I_{9/2}$, is stable and the $^4F_{3/2}$ state is meta-stable. The meta-stability means that it has a considerably longer lifetime than any other excited state, but will eventually decay to a lower state. The $^4F_{3/2}$ state lifetime in the Nd-fibers used in this experiment is approximately 405 μs. The other excited states all decay very rapidly, usually via phonons, to either the ground state or the $^4F_{3/2}$ state, if they have greater energy. The following figure illustrates Nd's electron energy states.

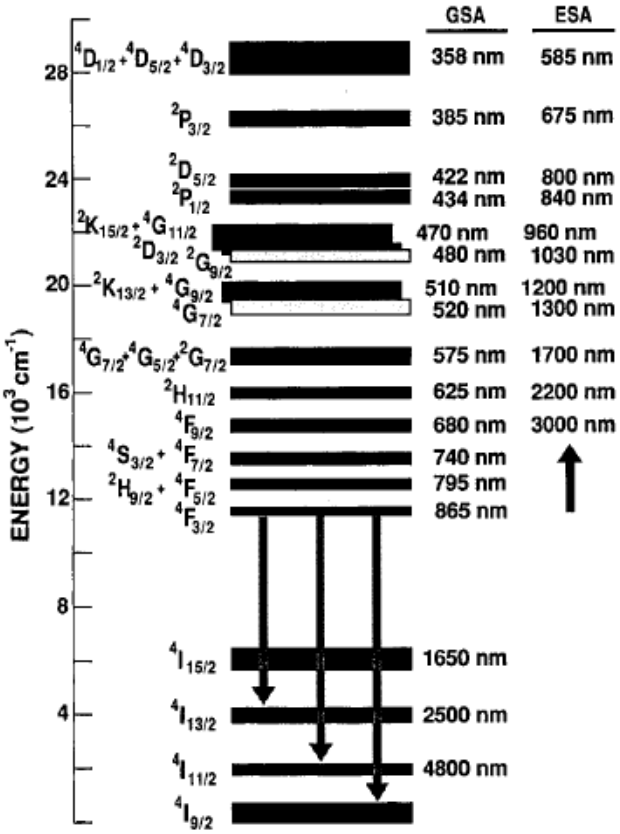

Figure 3: Energy level structure with GSA and ESA transition wavelengths for Nd in ZBLAN fluorozirconate [Miniscalco, 2001].

The numbers immediately to the right of the energy levels are the peak wavelengths for absorption from the ground state. To the right of those numbers are the peak wavelengths for excited state absorption from the $^4F_{3/2}$ state. The energy units of cm^{-1} are used on the energy scale on the left side of the figure. By taking the inverse of the energy, in these units, the wavelength of a photon (in cm) with that energy is obtained. In conventional energy units, 10^3 cm^{-1} is equivalent to 1.986 $x10^{-20}$ J or 0.124 eV.

These peak values will be slightly shifted to longer wavelengths in silica glass due to what is known as the nephelauxetic effect [Martin, 2006]. This effect is a result of the covalent bonding of the Nd atoms with the host material. This bonding lowers the energy levels, which corresponds to longer wavelengths. In spite of this, however absorption can still expected near these regions. The three downward arrows correspond to emission from the $^4F_{3/2}$ state, from left to right, at 1340 nm, 1064 nm, and 946 nm. The stimulated emission cross section for the transition at 1340 nm is shown below for Nd in various hosts.

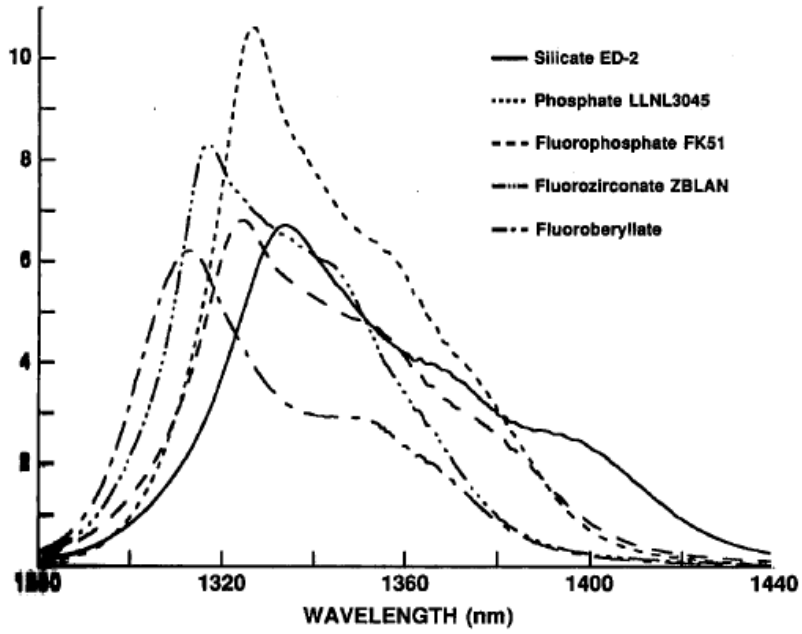

Figure 4: The emission cross section in units of 10^{-21} cm^2 for Nd in a variety of glass hosts [Miniscalco, 2001].

As can be seen from the graph, the peak of the emission cross section has been shifted to the right in silicate glass. Additionally, there is still noticeable emission at 1400 nm extending out to 1440 nm. This is important due to excited state absorption around 1300 nm, which we can expect based on the energy level diagram in Figure 3. The contribution of the ground state absorption will not be a factor in the region around 1400 nm, demonstrated in the figure below.

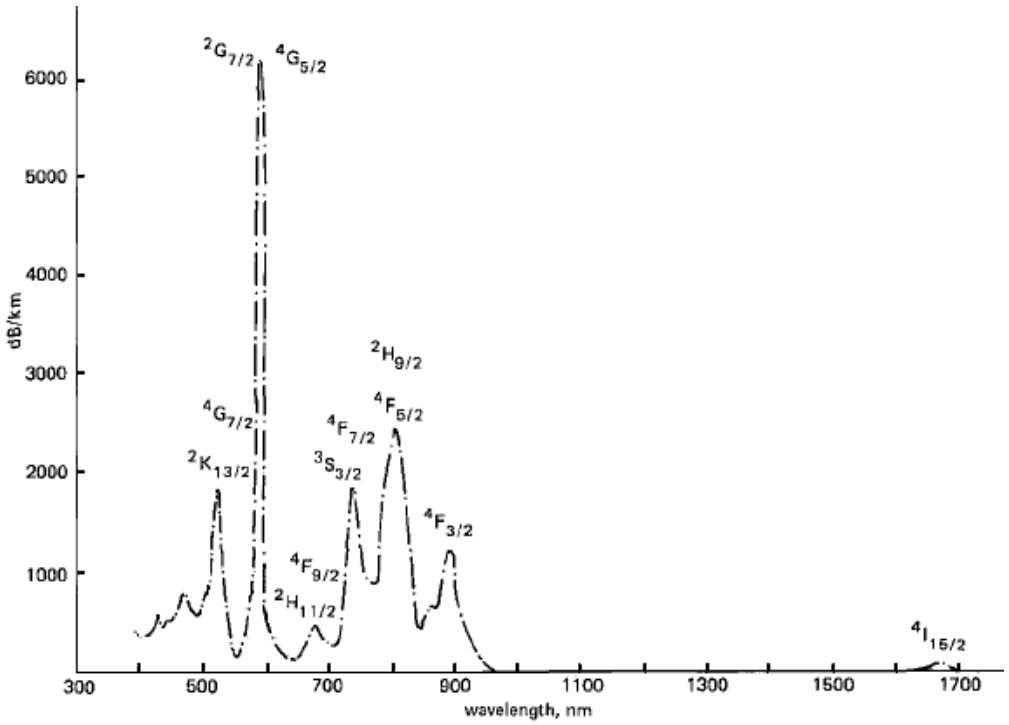

Figure 5: The ground state absorption of neodymium in silica glass, in dB/km. The doping concentration for this sample was 3.68×10^{17} cm^{-3} [Ainslie et al, 1988].

Using this figure, it is possible to estimate the ground state absorption cross section at 532 nm, the pump wavelength, as approximately 3.75×10^{-21} cm^2. Additionally, no ground state absorption is expected between 1000 and 1600 nm, leaving only the contributions of emission and excited state absorption in the pump probe measurement results.

2.3 Two Level Rate Equation

In neodymium, the ground energy state is stable and the $^4F_{3/2}$ state is meta-stable and electrons in any other state will rapidly decay to one of these two. For this reason, it can be assumed that the sum of the number of ions in the ground state and the number of ions in the $^4F_{3/2}$ state is always equal to the total number of neodymium ions.

$$N = N_1 + N_2 \tag{2.3-1}$$

This represents the assumption mentioned above, where N represents the total number of ions per unit volume, N_1 is the number of ions in the ground state per unit volume, and N_2 is the number of ions in the $^4F_{3/2}$ state per unit volume. To make the calculations

independent of sample size, all populations will be written in terms of population per unit volume. The excited state and ground state populations can then be related by the following expression:

$$N - N_2 = N_1 \tag{2.3-2}$$

An equation for the population of the excited state in the pumped case can now be constructed. Since the two states are linked by the above equation, writing a rate equation for each state is unnecessary. First, for the excited state, ions are pumped into the $^4F_{3/2}$ state via a laser at a rate of W_p. Ions can also be excited through ground state absorption of the input signal. However, only photons with a wavelength shorter than 900 nm will have enough energy to raise an electron to the $^4F_{3/2}$ state, otherwise the ion would immediately decay back to its ground state. Since it is safe to assume the pump power of the laser is much greater than the power of the input signal, the ground state absorption of the input signal, with regards to the overall excited state population change, can be ignored.

The excited state population decreases when an ion in the $^4F_{3/2}$ state decays. There are a number of possible energy levels the ion can decay to, each with its own transition probability, however once it reaches any of those states it will rapidly decay to the ground state. The ion can decay as a result of either stimulated or spontaneous emission. Once again, however, with a weak input signal, the stimulated emission case can also safely be ignored in the context of the rate equation. The $1/\tau_2$ term in the equation below represents the probability of an ion decaying from the excited state via spontaneous emission.

$$\frac{dN_2}{dt} = N_1\left(W_p + W_{gsa}\right) - N_2\left(\frac{1}{\tau_2} + W_{se}\right) \tag{2.3-3}$$

Equation 2.3-3 represents the rate equation including the terms representing ground state absorption and stimulated emission of the input signal. These two processes are represented by the rates W_{gsa} and W_{se} respectively. Ignoring these terms, a simpler version of the rate equation is obtained.

$$\frac{dN_2}{dt} = N_1 W_p - N_2 \frac{1}{\tau_2} \tag{2.3-4}$$

Measurements will be conducted in the steady-state situation, and therefore we can set the rate of population change equal to zero. This condition, along with equation 2.3-2, yields the following result:

$$NW_p = N_2 W_p + N_2 \frac{1}{\tau_2}$$

$$N_2 = N \frac{W_p}{W_p + \frac{1}{\tau_2}} \tag{2.3-5}$$

By multiplying top and bottom by the state lifetime, equation 2.3-5 appears as follows:

$$N_2 = N \frac{W_p \tau_2}{W_p \tau_2 + 1} \tag{2.3-6}$$

This equation provides an expression for the excited state population per unit volume, as a function of the total ion density, the pump rate, and the spontaneous emission lifetime.

The pump rate can be expressed in terms of ground state absorption cross section, σ_{gsa} the pump intensity, I_p, the pump frequency, v_p and Planck's constant, h. The rates for ground state absorption and stimulated emission can be written in a similar fashion by substituting the relevant cross section and replacing the intensity and frequency of the pump laser with the intensity and frequency of the input signal.

$$W_p = \frac{\sigma_{gsa} I_p}{h \upsilon_p} \tag{2.3-7}$$

The probability of spontaneous emission can be expressed in terms of the Einstein A coefficient. A_{2i} is the probability that an electron will spontaneously emit a photon and decay from the $^4F_{3/2}$ state (which we represent with the index '2') to a lower state with index 'i'. Each transition has its own probability; however the net probability for an ion to spontaneously emit a photon can be expressed as the sum of all the individual probabilities.

$$\frac{1}{\tau_2} = \sum_i A_{2i} = A_2 \tag{2.3-8}$$

2.4 Ground State Absorption Calculation

The absorption coefficient, α, multiplied by a path length, Δz, is defined as the fractional decrease in the intensity of a beam of light over that length. When the sample is in the ground state, and there are no emission processes occurring to increase signal strength, this relationship can simply be written as follows.

$$\frac{I_2 - I_1}{I} = -\alpha(z_2 - z_1)$$

When the path length approaches zero, the differences in the above equation can be replaced with differential values.

$$\frac{dI}{I} = -\alpha(dz) \tag{2.4-1}$$

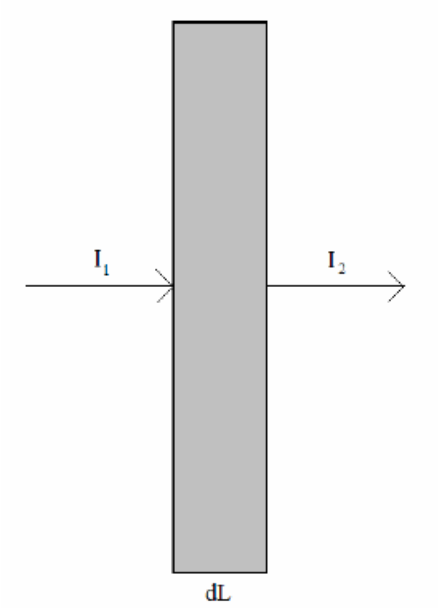

Figure 6: Diagram showing change in intensity over differential path length dL

In equation 2.4-1, it is important to note that the absorption coefficient is not a constant; it can vary with respect to position, wavelength, and even time if the sample is not in thermal equilibrium. The absorption coefficient can also be expressed as the absorption cross section of a single particle multiplied by the number density of absorbing particles per unit volume.

$$\alpha = N\sigma$$

The cross section, while dependent on wavelength, is a property of an individual ion in a medium and is invariant over the length of a sample; however the number density of absorbing particles is not. The possible variation that is relevant to this study is when a relatively strong pump beam creates a significant change in the number of ions in an excited state. As the pump beam is absorbed over the length of the sample, the number of ions in the excited state decreases. As mentioned in Section 2.1, an excited ion can also absorb light; however it will have a different cross section.

In the special case of an un-pumped sample and a relatively weak probe beam, the absorption coefficient corresponds only to the ground state absorption. Both sides of equation 2.4-1 can be integrated over the length of the sample.

$$\ln(I)\Big|_{I_0'}^{I(z)} = -\alpha z'\Big|_0^z$$

$$\ln(I(z)) - \ln(I_0') = -\alpha z$$

$$\ln\left(\frac{I(z)}{I_0'}\right) = -\alpha z \tag{2.4-2}$$

In the above equation, *I(z)* is the intensity of the signal at position *z* and *I'0* is the intensity at *z=0*, called the 'launched' intensity. Not all of the light that is incident on the sample will be either absorbed or transmitted. Some is reflected at the surface of the sample and some is scattered. For this reason, in the absorption equation, the incident signal is multiplied by an additional factor.

$$I_0' = I_0\left(1 - \Re^2\right)f_s$$

In this expression, I_0 represents the intensity of the signal incident on the sample. This can then be plugged into equation 2.4-2 and both sides can be exponentiated.

$$I(z) = I_0\left(1 - \Re^2\right)f_s e^{-\alpha z} \tag{2.4-3}$$

This equation is commonly known as Beer's Law. For ease of calculation, *R* will denote the combination of the scattering and reflection terms. The absorption coefficient can also be replaced with the cross section and number density. Beer's Law can then be re-written as follows.

$$I(z) = RI_0 \exp\left(-\sigma_{gsa} N z\right) \tag{2.4-4}$$

The *gsa* subscript above indicates the cross section is for ground state absorption.

In this experiment, it will be possible to directly measure the incident signal intensity, the final intensity of the signal after it has exited the fiber (I_f), and the length of the fiber. Therefore, $z=L$ will be plugged into Equation 2.4-4 and the absorption coefficient will be solved for.

$$\sigma_{gsa} = \frac{1}{NL}\ln\left(\frac{RI_0}{I_f}\right) = \frac{1}{NL}\left[\ln\left(\frac{I_0}{I_f}\right) + \ln(R)\right] \tag{2.4-5}$$

The signal intensities vary with wavelength, often with sharply defined features. The reflection term, however, varies relatively slowly. Therefore, data from regions where we know the ground state absorption coefficient of the sample is zero can be used to determine the contribution of R. This contribution can then be subtracted, leaving the ground state absorption cross section.

2.5 Absorption in the Pumped Case

It is possible to obtain the excited state absorption cross section by beginning with a derivation similar to what was used for Beer's Law. The fractional change in intensity over a short path length is written in terms of an absorption coefficient, α, and a gain coefficient, γ, multiplied by the path length.

$$\frac{\Delta I}{I} = (\gamma - \alpha)\Delta z \tag{2.5-1}$$

When the change in length becomes very small, it is possible to integrate the expression.

$$\int \frac{dI}{I} = \int (\gamma - \alpha) dz \tag{2.5-2}$$

In the un-pumped case, there is no gain and the absorption coefficient can be readily obtained after a baseline extrapolation has performed based on measurements of the input signal and the signal after it has passed through the sample. The absorption coefficient is

simply equal to the total number density of ions multiplied by the ground state absorption cross section.

In the pumped case, the gain coefficient is equal to the number density of ions in the excited state multiplied by the stimulated emission cross section. The absorption coefficient is equal to the ground state absorption cross section multiplied by the number density of ions in the ground state plus the excited state absorption cross section multiplied by the number density in the excited state.

$$\begin{aligned} \gamma &= N_2\sigma_{se} \\ \alpha &= N_2\sigma_{esa} + N_1\sigma_{gsa} \end{aligned} \tag{2.5-3}$$

The pump signal is absorbed as it passes through the fiber, and therefore the pump intensity varies with position ('z' will be used as the axis parallel to the axis of the fiber), which means the pump rate varies with z, as does the excited population. Since the absorption and gain coefficients both depend on the excited state population, they vary with z as well.

$$\begin{aligned} \int_{I_0'}^{I_L'} \frac{dI'}{I'} &= \int_0^L \left[-\sigma_{gsa}\left(N - N_2(z)\right) - \sigma_{esa}N_2(z) + \sigma_{se}N_2(z)\right]dz \\ \int_{I_0'}^{I_L'} \frac{dI'}{I'} &= \int_0^L \left[-\sigma_{gsa}N + \left(\sigma_{se} + \sigma_{gsa} - \sigma_{esa}\right)N_2(z)\right]dz \end{aligned} \tag{2.5-4}$$

It is then possible to evaluate the integral on the left hand side and simplify the right hand side by pulling out terms that do not depend on z.

$$\ln\left(I_f\right) - \ln\left(RI_0\right) = -\sigma_{gsa}NL + \left(\sigma_{gsa} + \sigma_{se} - \sigma_{esa}\right)\int_0^L N_2(z)dz \tag{2.5-5}$$

In the above expression, the reflection term, R, and the intensities are defined in the same way as in the previous section. An average excited state population can be defined in order to simplify the equation.

$$\overline{N}_2 = \frac{1}{L}\int_0^L N_2(z)dz \tag{2.5-6}$$

Plugging into equation 2.5-5:

$$\ln\left(\frac{I_f}{I_0}\right)-\ln(R)=-\sigma_{gsa}NL+\left(\sigma_{gsa}+\sigma_{se}-\sigma_{esa}\right)\overline{N}_2L \tag{2.5-7}$$

If the pump light were switched off, equation 2.5-7 would instead appear as follows:

$$\ln\left(\frac{I_f^u}{I_0}\right)-\ln(R)=-\sigma_{gsa}NL \tag{2.5-8}$$

In this case, the index *u* has been added to the measured intensity to indicate this is the measured signal in the un-pumped case. In further calculations, the index *p* will also be added to the pumped cases.

Next, Equation 2.5-8 will be subtracted from Equation 2.5-7.

$$\left(\ln\left(\frac{I_f^p}{I_0}\right)-\ln(R)\right)-\left(\ln\left(\frac{I_f^u}{I_0}\right)-\ln(R)\right)=\left(-\sigma_{gsa}NL+\left(\sigma_{gsa}+\sigma_{se}-\sigma_{esa}\right)\overline{N}_2L\right)-\left(-\sigma_{gsa}NL\right)$$

$$\ln\left(\frac{I_f^p}{I_0}\right)-\ln\left(\frac{I_f^u}{I_0}\right)=\left(\sigma_{gsa}+\sigma_{se}-\sigma_{esa}\right)\overline{N}_2L$$

$$\ln\left(\frac{I_f^p}{I_f^u}\right)=\left(\sigma_{gsa}+\sigma_{se}-\sigma_{esa}\right)\overline{N}_2L \tag{2.5-9}$$

This provides an expression that equates the log of the ratio of two quantities that will be measured during the experiment with a constant scaling factor multiplied by the cross sections. The ground state absorption cross section can be calculated using Beer's Law and measurements of the incident and transmitted signals in the un-pumped case. The stimulated emission cross section must then be determined by using fluorescence data, to be discussed in Section 2.6.

2.6 Calculation of Stimulated Emission from Fluorescence

The stimulated emission cross section can be determined based on the spontaneous emission spectrum [McCumber 1964].

$$f_\lambda(\omega)=\sigma_{se}\left[\frac{n(\lambda)\omega}{2\pi c}\right]^2 \tag{2.6-1}$$

$$A_2 = \sum_{\lambda} \int_{4\pi} d\Omega_{k\lambda} \int \frac{d\omega}{2\pi} f_{\lambda}(\omega)_2 \tag{2.6-2}$$

In the above equations, *n(λ)* represents the index of refraction of the sample medium, *ω* is the angular frequency of a photon, *c* is the speed of light, and *f* is the number of photons emitted each second per unit frequency interval per solid angle. The spontaneous emission probability, A_2, from the excited state is the integral of the function *f* over the entire frequency range and all solid angles, spanning 4π steradians. The data collection apparatus used in this study collects spectra as a function of wavelength, and therefore it is necessary to convert Equation 2.6-1 into an expression in terms of wavelength.

$$\begin{aligned} \omega &= \frac{2c\pi}{\lambda} \\ d\omega &= \frac{2c\pi}{\lambda^2} d\lambda \end{aligned} \tag{2.6-3}$$

The above relationships between angular frequency and wavelength can be plugged into the fluorescence equation with an arbitrary frequency interval.

$$\begin{aligned} f_{\lambda}(\omega)\frac{d\omega}{2\pi} &= \sigma_{se}\left[\frac{n(\lambda)\omega}{2\pi c}\right]^2 \frac{d\omega}{2\pi} \\ f_{\lambda}(\lambda)d\lambda &= f_{\lambda}(\omega)\frac{d\omega}{2\pi} \\ f_{\lambda}(\lambda)d\lambda &= \sigma_{se}\left[\frac{n(\lambda)}{2\pi c}\frac{2c\pi}{\lambda}\right]^2 \frac{1}{2\pi}\frac{2c\pi}{\lambda^2} d\lambda \\ f_{\lambda}(\lambda) &= \frac{\sigma_{se} c n^2(\lambda)}{\lambda^4} \end{aligned} \tag{2.6-4}$$

The equipment used to collect data for this experiment measures optical power over a short wavelength interval, not the number of incident photons. Therefore the probability a photon will be emitted must be multiplied by the energy of the photon. As can be seen from equation 2.6-2, the total probability a photon will be emitted is equal to the integral of the function *f* over solid angle and frequency interval. The assumption will be made that photons are emitted uniformly in all directions, and therefore the solid angle integral simply becomes the solid angle spanned by the collection lens, Ω. It is possible to approximate the wavelength integral over a small range by simply multiplying the function *f* by the wavelength interval.

$$\Delta P(\lambda) = N_2 \frac{hc}{\lambda} \Omega f_\lambda(\lambda) \Delta\lambda = h\sigma_{se}\Omega\left[\frac{c^2 n^2(\lambda)}{\lambda^5}\right]\Delta\lambda \tag{2.6-5}$$

In this expression, ΔP(λ) represents the measured optical power over the wavelength range Δλ, as a function of wavelength. This wavelength range is determined by the slit width on the scanning monochrometer. Equation 2.6-5 can then be solved for the stimulated emission cross section.

$$\sigma_{se} = \frac{\Delta P(\lambda)\lambda^5}{c^2 n^2(\lambda) h\Omega\Delta\lambda} \tag{2.6-6}$$

Since the overall magnitude of the emission cross section will be scaled using the Judd-Ofelt procedure discussed in Section 2.7, only the spectral shape of the cross section is important. Therefore, a simpler form of Equation 2.6-6 using only the terms that can vary with wavelength can be written as follows:

$$\sigma_{se} \propto \frac{\Delta P \lambda^5}{n^2} \tag{2.6-7}$$

2.7 Judd-Ofelt Procedure and Oscillator Strengths

The oscillator strength and the total integrated cross section of an optical transition can be estimated using the Judd-Ofelt method. The Judd-Ofelt method utilizes three parameters (Ω_2, Ω_4, and Ω_6), which vary with the dopant ion, Nd or Er in this case, and the host material, silica glass. These parameters are tabulated [Gschnieder et al, 1998], or can be determined empirically from ground state absorption measurements. The Judd-Ofelt method is an approximation with an uncertainty of 10-20%.

The oscillator strength between two levels is the sum of an electric dipole term and a magnetic dipole term.

$$f = f_{ed} + f_{md} \tag{2.7-1}$$

The emission oscillator strength for the transition between two levels is equal to the absorption oscillator strength multiplied by the ratio of the degeneracies of the two states.

$$f_{emit} = \frac{g_1}{g_2} f_{abs} \tag{2.7-2}$$

In Equation 2.7-2, g_1 represents the degeneracy of the lower energy state, and g_2 is the degeneracy of the upper energy state. Each energy level is 2J+1 fold degenerate, where J is the quantum number L+S. Since all of the energy states discussed in this report are written in the standard spectroscopic notation, $^{2S+1}L_J$, it is simple to determine the degeneracies of the states.

The electric dipole oscillator strength can be calculated from the Judd-Ofelt parameters and the following equation:

$$f_{ed} = \frac{8\pi^2 mc\chi_{ed}}{3h\lambda(2J_i+1)n^2} \sum_{t=2,4,6} \Omega_t \left|\left\langle a\left\|U^t\right\|b\right\rangle\right|^2 \tag{2.7-3}$$

$$\text{Where} \quad \chi_{ed} = \frac{n(n^2+2)^2}{9}$$

In the above equation, m is the mass of an electron, c is the speed of light, h is Planck's constant, λ is the wavelength of a photon with energy equal to the difference between the two levels, J_i is the J quantum number of the initial state, and n is the index of refraction in the medium. The quantity $\left\langle a\left\|U^t\right\|b\right\rangle$ is the doubly reduced matrix element of the tensor operator U^t between the two levels, a and b. These matrix elements for neodymium and erbium have been tabulated [Carnall et al, 1977].

Calculation of the magnetic dipole oscillator strength does not require the use of the Judd-Ofelt parameters. Instead of the tensor operator, the sum of the angular momentum operator and twice the spin operator is used.

$$f_{md} = \frac{hc\chi_{md}}{6\lambda(2J_i+1)n^2mc^2} \left|\left\langle a\left\|L+2S\right\|b\right\rangle\right|^2 \tag{2.7-4}$$

$$\text{Where} \quad \chi_{md} = n^3$$

The magnetic dipole term is only significant for a limited number of the possible transitions due to two selection rules. The first is that the initial and final states must have the same L quantum number; and the second is that the change in the J quantum number

must be zero or positive/negative 1. Of all the neodymium and erbium energy level transitions that will be observed in this study, only the erbium transition between the $^4I_{15/2}$ and $^4I_{13/2}$ states will have a magnetic dipole contribution (see Section 2.8 for the erbium energy level structure). The magnetic dipole oscillator strengths for relevant transitions are tabulated [Carnall et al, 1968 (2)].

Once the oscillator strength of a certain transition is known, the total integral of the cross section can be calculated. It is important to note that only the integral, not the spectral shape of the cross section, can be found using this method.

$$f = \frac{4\varepsilon_0 mc}{e^2}\int \sigma(\nu)d\nu \tag{2.7-5}$$

In the above expression, f represents the oscillator strength of the transition in question, e is the charge of an electron, ε_o is the permitivity of free space, ν is frequency, and σ is either the absorption or emission cross section, depending on the transition. Equation 27-5 can be re-written in terms of wavelength and solved for the cross section integral. It is then possible to apply equation 2.7-1 to obtain an expression for the integrated absorption or emission cross section between two energy levels.

$$\int \sigma(\lambda)\frac{c}{\lambda^2}d\lambda = \frac{e^2}{4mc\varepsilon_0}\left(f_{ed} + f_{md}\right) \tag{2.7-6}$$

When using the above equation, it is important to keep in mind that the electric dipole oscillator strength is not the same for emission between two levels as it is for the absorption between the same two levels, since the initial J quantum number is used in the calculation. These calculated integrals can be used to determine the scale of the emission spectra measured in the lab, yielding a cross section with the correct spectral shape and magnitude.

2.8 Erbium Characteristics

Like neodymium, erbium is a rare-earth element commonly used in optical systems. Erbium has only one emission band, at 1530 nm, and is widely used in fiber

amplifiers for this wavelength. The energy band structure of erbium is displayed in the figure below.

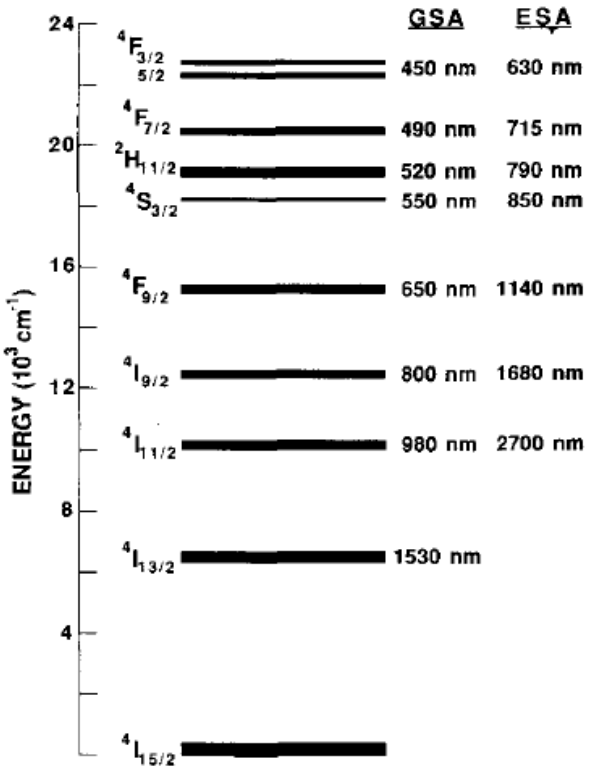

Figure 7: Erbium energy level structure with GSA and ESA transition wavelengths labeled [Miniscalco, 1991].

With the exception of the ground state, the only Er energy level with a long enough lifetime to sustain a significant population is the $^4I_{13/2}$ state. Electrons in any other energy levels above the $^4I_{13/2}$ state will rapidly decay to this state via non-radiative means, from which the electrons will decay via the 1500 nm transition to the ground state.

Due to erbium's elementary energy structure and its well-documented spectra, an erbium-doped optical fiber will be used in the same experimental configurations as the neodymium-doped fiber in order to verify the efficacy of the data collection methods used in this study.

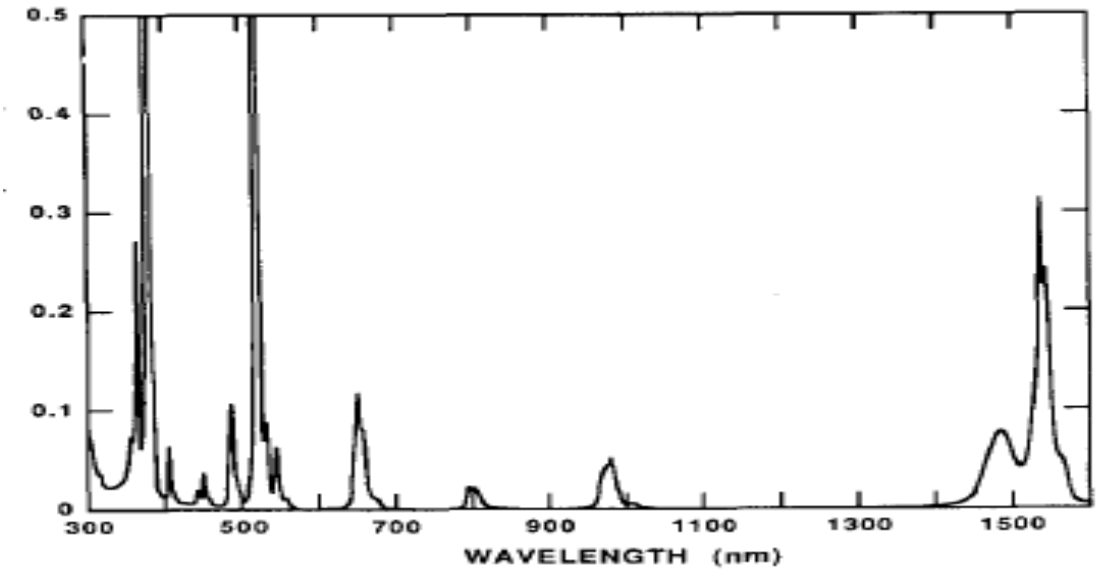

Figure 8: The ground state absorption coefficient, in arbitrary units, of erbium-doped L22 silica glass [Miniscalco, 1991].

In the experiments conducted for this project, a laser operating at 532 nm will be used as the pump source. In Figure 8 a large peak at a wavelength above 500 nm can be observed, and by consulting Figure 7 it is clear this is the 520 nm absorption transition. This peak decreases very rapidly; therefore, a large excited state population is not expected due to non-optimal pump absorption.

2.9 Blackbody Radiation

A blackbody is defined as an object that perfectly absorbs light of all wavelengths, meaning no light is reflected (hence the 'black' in the name). When a blackbody is heated to a certain temperature, it emits the same spectrum it would absorb if it were in a uniform environment at that temperature. This spectrum is independent of the material and varies only with temperature.

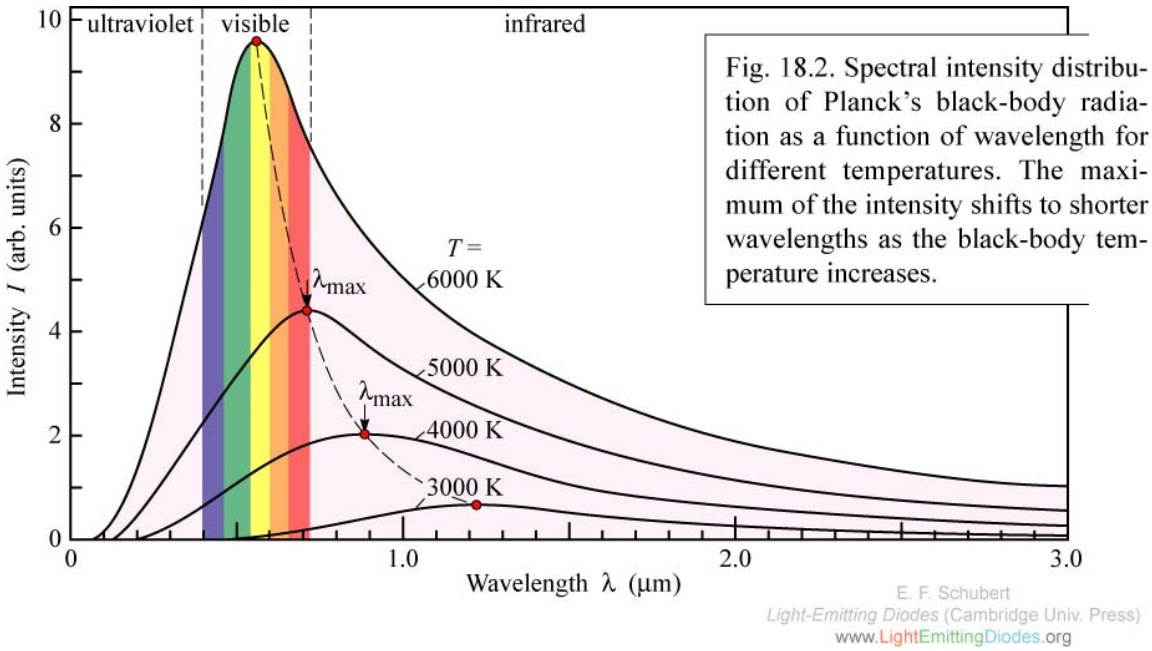

Figure 9: Ideal blackbody radiation curves for various temperatures [Schubert, 1993].

The curves shown above are generated from Planck's Law of Blackbody Radiation.

$$\rho(\nu) = \frac{8\pi h \nu^3}{c^3} \frac{1}{\exp\left(\frac{h\nu}{k_B T}\right) - 1} \tag{2.9-1}$$

This function is the spectral energy density of a blackbody emitter, meaning that it is the energy radiated as a function of frequency, per unit volume and unit frequency interval. In the above equation, h is Planck's constant, k_B is Boltzmann's constant, c is the speed of light, T is the temperature in Kelvin, and ν is the frequency. In order to match the data collected in this experiment, and the graph shown above, Equation 2.9-1 must be converted to wavelength using the following relationships.

$$\nu = \frac{c}{\lambda}$$

$$d\nu = \frac{c}{\lambda^2} d\lambda$$

These relationships can be plugged into the Planck distribution for an arbitrary frequency interval.

$$\rho(\nu)d\nu = \frac{8\pi h\nu^3}{c^3}\frac{1}{\exp\left(\frac{h\nu}{k_B T}\right)-1}d\nu$$

$$\rho(\lambda)d\lambda = \frac{8\pi h}{\lambda^3}\frac{1}{\exp\left(\frac{hc}{k_B T\lambda}\right)-1}\frac{c}{\lambda^2}d\lambda = \frac{8\pi hc}{\lambda^5}\frac{1}{\exp\left(\frac{hc}{k_B T\lambda}\right)-1}d\lambda \qquad (2.9\text{-}2)$$

By differentiating, it is possible to obtain a simple relationship between the peak wavelength value and the temperature of the blackbody. This relationship is known as Wien's Displacement Law.

$$\lambda_{\max} T = 2.8977685\times 10^6\, nm\cdot K \qquad (2.9\text{-}3)$$

Where T is the temperature in Kelvin, and λ_{max} is the peak wavelength.

Using these two relationships, the spectrum of the tungsten bulb, collected by the Optical Spectrum Analyzer (see Appendix B), can be compared with an ideal blackbody radiator.

2.10 Tungsten Bulb Calibration

The spectral data for this experiment will be collected using a germanium photodetector and a scanning monochrometer utilizing a rotatable diffraction grating. Since neither the detector nor the diffraction grating is equally efficient at all wavelengths, it will be necessary to calibrate the observed data in order to obtain the correct spectral shape. The emission spectrum of the tungsten bulb is very close to what would be expected of an ideal blackbody at 2900 K [Martin, 2006]. Since the Planck distribution, discussed in the previous section, mathematically represents the blackbody radiation spectrum it is possible to use the tungsten bulb to determine the responsivity of the detector-grating combination as a function of wavelength.

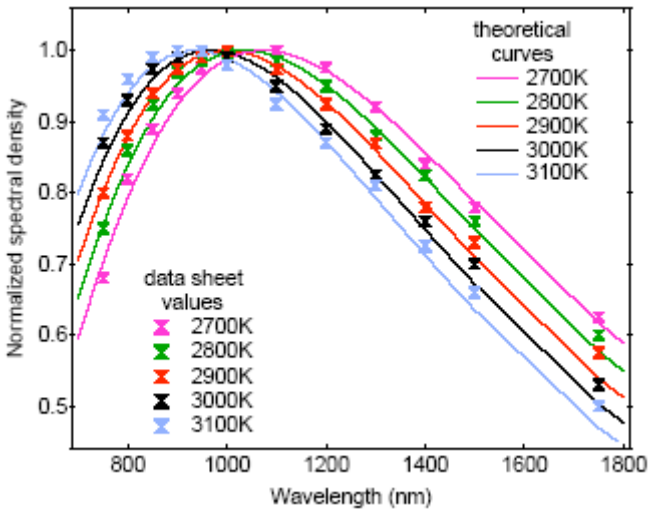

Figure 10: Theoretical blackbody radiation curves plotted in comparison to the measured tungsten bulb spectra at a range of temperatures [Martin, 2006].

As demonstrated in Figure 10, the tungsten bulb spectral shape is very close to that of an ideal blackbody. At wavelengths above and below the peak value, however, the values for the tungsten bulb become marginally greater than the ideal curve. The emission data collected must be scaled by either using the Judd-Ofelt method previously discussed, or graphically from pump-probe measurements. Therefore only the rate of change of the calibrated spectrum is required, not the absolute value. For this reason, when considering spectral scans over shorter wavelength intervals, the slight offset between the bulb spectra and the ideal blackbody curves will not affect the calibrated emission spectra. In erbium, there is only one emission peak and therefore it can be assumed that the bulb is a blackbody emitter. In neodymium, on the other hand, there are three peaks, between 900 and 1350 nm. When comparing the measured oscillator strengths of the different peaks with larger wavelength intervals in between them, some error may be introduced due to differences between the tungsten bulb spectrum and the predicted blackbody radiation curve.

2.11 OH ion absorption

Hydroxyl ions (OH^-) are commonly found as a contaminant mixed in with the glass host in optical fibers. This is largely due to any ambient humidity present during the fabrication process. This has the effect of causing additional attenuation of light passing

through the fiber in the near-infrared wavelength range. The figure below demonstrates the difference between the attenuation of an optical fiber with OH^- ions present and the theoretical losses due to Rayleigh scattering and lattice vibrations.

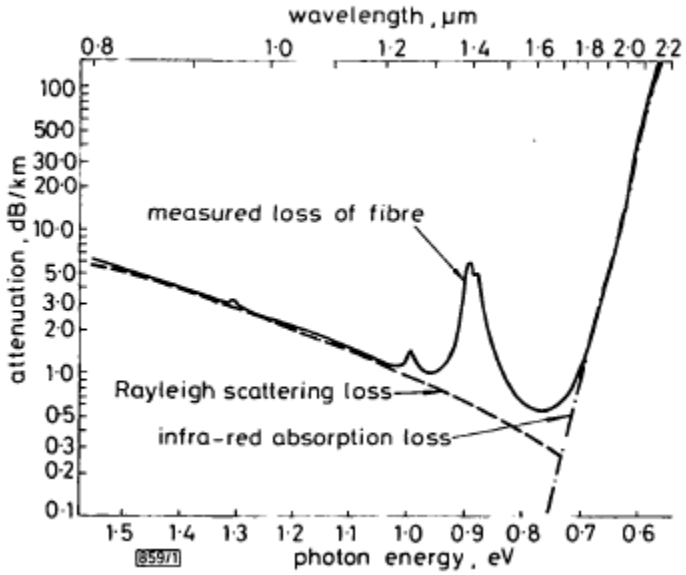

Figure 11: Attenuation of a SiO_2/GeO_2 fiber compared with theoretical Rayleigh scattering and IR losses [Belov et al, 1982].

For wavelengths below 1200 nm and above 1800 nm, the actual attenuation of the fiber matches the predicted value, however between theses values there is a clear discrepancy. The OH^- ion absorption peak occurs at a wavelength just below 1400 nm. The overall magnitude of the attenuation depends upon the conditions in which the optical fiber was created and how many hydroxyl ions are present in the sample. For this study, neither Nd nor Er is predicted to absorb at 1400 nm and therefore it should be possible to isolate this effect.

3. Methodology

3.1 Equipment Set-up

The Jarrell-Ash scanning monochrometer will be the primary apparatus used for data collection in this experiment. The monochrometer is used in conjunction with a photodector, a lock-in analyzer, and data collection software on the laboratory computer. The photodetector used in this experiment will be a germanium detector cooled with dry ice to a temperature of –78.5 C. The figure below illustrates the equipment set-up for measurements of light transmission through a sample fiber, in both the pumped and un-pumped cases.

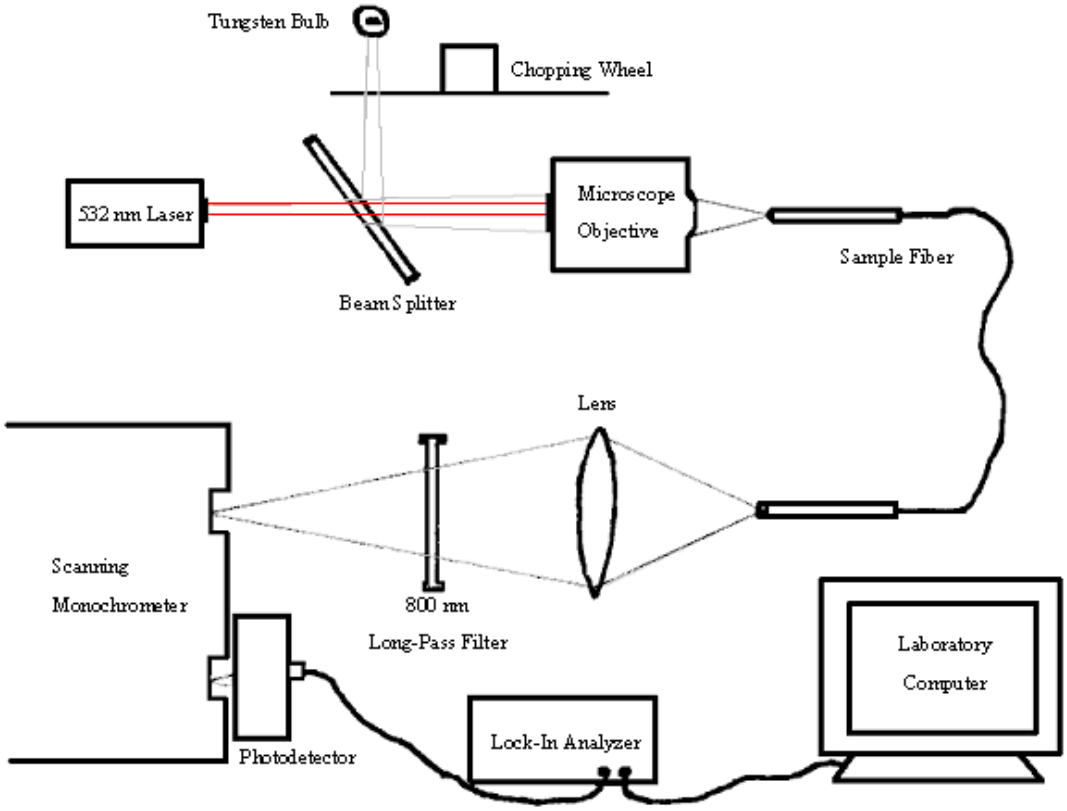

Figure 12: Experiment set-up for pump-probe measurements

Light from a tungsten bulb will be modulated with a chopping wheel before it is reflected off a beam splitter. The bulb light will then be coupled into the sample fiber using a microscope objective. A laser, operating at 532 nm, will be pass through the beam splitter and into the microscope objective as well. The laser will be switched off in the un-pumped case. The signal exiting the fiber will be collected by a lens, passed through

an 800 nm long pass filter to eliminate any pump light, and focused onto the input slit of the monochrometer.

Two additional measurements will be made using set-ups similar to what is pictured above. The bulb signal will also be measured directly by collecting the light from the bulb with a lens, passing it through the long-pass filter and chopping wheel, and focusing it directly on the input slit of the monochrometer. The transmission of the doped fiber will also be determined by coupling the bulb signal directly into the microscope objective without the use of a beam splitter.

Finally, fluorescence measurements must also be made. In this case, the laser is coupled directly into the sample fiber using the microscope objective. A lens is placed at 90 degrees to the axis of the fiber, close to where the laser is coupled in. This lens collects the light being emitted by the fiber in all directions from spontaneous emission. This collected light is passed through the 800 nm long-pass filter to eliminate the laser light that is scattered within the fiber. The signal is then modulated with the chopping wheel and incident on the input slit of the monochrometer.

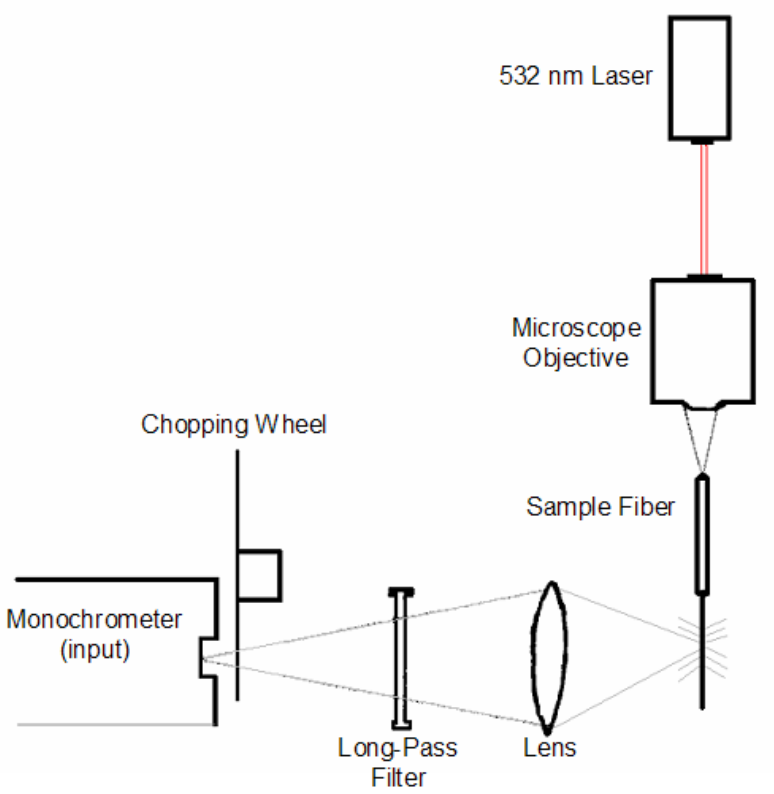

Figure 13: Set-up for fluorescence measurements

After the light from any of the above measurements described enters the monochrometer, it is reflected off of a rotatable diffraction grating. After the light is dispersed by the grating, only a narrow range of wavelengths of the input signal passes through the output slit. The size of this wavelength range is dependent on the slit size of the monochrometer. The speed at which the grating rotates can be varied to adjust the scan rate. After exiting the monochrometer, the light is incident on the Ge photodetector. The signal from the detector is then biased with a resistor, depending on signal strength, and sent to the lock-in analyzer. The lock-in filters out any signals with a frequency different than that of the reference frequency, supplied by the chopping wheel. The range of frequencies accepted can be varied by changing the time constant. Depending on signal strength, the lock-in can be set to different sensitivities and can amplify either the incoming or outgoing signal if necessary. Finally, the signal from the lock-in analyzer is sent to the lab computer and collected as a function of wavelength.

3.2 Data Collection Procedures

Five separate measurements will be taken to gather the data required to obtain an excited state absorption spectrum. The same measurements will be taken for both the erbium and neodymium-doped optical fibers, and each measurement will be repeated six times. The results of the six scans will be averaged in an effort to improve the signal-to-noise ratio. All of the scans below will be conducted using the same scan range, 800-1600 nm, and the data points will be 0.5 nm apart. Additionally, the modulation frequency of 95 Hz will be used in each of the scans.

The spectrum of the tungsten bulb was collected by focusing the light from the bulb through the 800 nm long-pass filter and chopping wheel, then directly onto the input slit of the monochrometer. The following parameters were used during these scans:

Tungsten Bulb Spectrum	
Light Source	tungsten bulb
Lock-In Sensitivity	1 mV
Bias Resistance	2 kΩ
Lock-In Time Constant	1 s
Scan Rate	25 nm/min

Table 1: The scan parameters used when measuring the tungsten bulb spectrum.

The resulting spectrum was used as a reference for the fiber transmission measurements and a basis for determining the responsivity of the diffraction grating/Ge detector combination.

The tungsten bulb was coupled into the doped fibers to measure the fraction of light transmitted through the fibers. The bulb was placed approximately 30 nm from the microscope objective used to focus the light into the ‘front end’ of the fiber. The other end of the fiber was placed facing a silicon photodetector shielded from any ambient light. The position of the ‘front end’ of the fiber was adjusted by maximizing the signal from the Si detector. Once this was complete, the light exiting the fiber was collected using a lens, passed through the chopping wheel and long-pass filter, and into the monochrometer. During the data collection, the following scan parameters were used:

Fiber Transmission		
Parameter	**Er Fiber**	**Nd Fiber**
Light Source	tungsten bulb	tungsten bulb
Lock-In Sensitivity	250 μV output x10	250 μV output x10
Bias Resistance	900 kΩ	900 kΩ
Lock-In Time Constant	1 s	1 s
Scan Rate	25 nm/min	25 nm/min

Table 2: The scan parameters used when measuring the transmission through the doped fibers.

The 'output x10' refers to the amplification of the signal measured using the lock-in analyzer.

The fluorescence spectrum was observed by measuring the light being emitted by the doped fibers perpendicular to the fiber axis. The laser was incident directly onto the microscope objective and focused into the optical fiber. The coupling was maximized in the same manner outlined above. The scan parameters used for these measurements are listed in the table below.

Fluorescence		
Parameter	**Er Fiber**	**Nd Fiber**
Light Source	532 nm laser	532 nm laser
Lock-In Sensitivity	100 μV output x10	100 μV output x10
Bias Resistance	12 MΩ	12 MΩ
Lock-In Time Constant	1 s	1 s
Scan Rate	25 nm/min	25 nm/min

Table 3: The scan parameters used when measuring the fluorescence of the doped fibers.

The final two measurements taken were the transmission of the doped fibers in the pumped and un-pumped configurations. The set-up for these scans is depicted in Figure 12. For the scans measuring the pumped and un-pumped transmission of the erbium-doped fiber, a neutral density filter with an optical density of 0.4 was used as the beam splitter. For the neodymium-doped fiber, the beam splitter had an optical density of 0.2.

$$T = 10^{-OD}$$
$$R = 1 - 10^{-OD} \qquad (3.2\text{-}1)$$

$$T_{0.4} = 10^{-0.4} = 0.398 \quad \text{and} \quad T_{0.2} = 10^{-0.2} = 0.631$$
$$R_{0.4} = 1 - 10^{-0.4} = 0.602 \quad \text{and} \quad R_{0.2} = 1 - 10^{-0.2} = 0.369$$

These equations relate the fraction of light transmitted, *T*, or reflected, *R*, as a function of the optical density, *OD*. The neodymium fiber, therefore, had a greater pump power compared to the erbium fiber since Nd absorbs more strongly at 532 nm and a greater population inversion was possible. The following scan parameters were used during the pump-probe measurements:

Pump-Probe Measurements		
Parameter	**Er Fiber**	**Nd Fiber**
Light Source	tungsten bulb	tungsten bulb
Lock-In Sensitivity	100 μV output x10	100 μV output x10
Bias Resistance	12 MΩ	12 MΩ
Lock-In Time Constant	3 s	10 s
Scan Rate	25 nm/min	10 nm/min

Table 4: The scan parameters used during the pump-probe measurements.

Finally, one additional scan was taken with both the laser and tungsten bulb blocked to determine the electrical offset of the data collection system.

3.3 Analysis Procedures

The ground state absorption cross section can be calculated from the fiber transmission and tungsten bulb measurements. After subtracting the electrical offset introduced by the data acquisition system, the average fiber transmission signal is divided by the reference signal of the bulb. Referring to Beer's Law (Section 2.4), this ratio is equivalent to a reflection term multiplied by the exponential of the negative fiber length multiplied by the doping concentration and absorption cross section.

$$\frac{I}{I_0} = R \cdot \exp\left(-\sigma_{gsa} NL\right) \tag{3.3-1}$$

Next, the natural log is taken of the ratio of transmitted over incident intensity.

$$\ln\left(\frac{I}{I_0}\right) = -\sigma_{gsa} NL + \ln(R) \tag{3.3-2}$$

The resulting data is then examined only in the regions in which no ground state absorption is expected (see Sections 2.2 and 2.8 for Nd and Er absorption spectra, respectively). A trend-line is fit to this data, and subtracted.

$$\ln\left(\frac{I}{I_0}\right) - \ln(R) = -\sigma_{gsa} NL \tag{3.3-3}$$

Finally, the data is divided by the negative length of the fiber, leaving the ground state absorption cross section multiplied by the doping concentration.

$$\frac{-1}{L}\left[\ln\left(\frac{I}{I_0}\right) - \ln(R)\right] = \sigma_{gsa} N \tag{3.3-4}$$

The exact doping concentrations of the erbium and neodymium fibers are not known. However, the absorption spectra of both have been well documented, and it is therefore possible to compare the peaks in the observed data with results found in the literature to determine the doping concentration of the optical fibers.

Ground State Absorption Cross Section							
A	B	C	D	E	F	G	H
Average Transmission	Average Bulb	(A-offset) / (B-offset)	ln(C)	D in regions where no GSA	Linear fit of E for all points	D - F	G / (*N* x *L*)

Table 5: An illustration of the data analysis methods used to calculate the ground state absorption cross section.

The above table illustrates the data calculations used to obtain the GSA cross section. The letter above each cell represents that value for use in other cells. For example 'ln(C)' is equivalent to the natural log of the average fiber transmission minus the electrical offset, divided by the average bulb spectrum minus the offset. In the final cell, however, N is the doping concentration and L is the length of the fiber.

Once a fluorescence spectrum is measured, it must be modified as discussed in Section 2.6 to obtain the stimulated emission cross section. Using the assumption that the index of refraction of the host glass changes very little over the wavelength range of the collected data, it is only necessary to multiply the measured fluorescence by a factor of λ^5 to obtain the proper shape.

$$\sigma_{se} \propto \Delta P \lambda^5 \tag{3.3-5}$$

The emission cross section must then be scaled using the Judd-Ofelt method, outlined in Section 2.7. In erbium, there is only one emission peak, but in neodymium there are three. The data must then be split into three separate pieces to isolate each peak. Once the peaks are separated, the approximate integral can be obtained by multiplying each data point by the distance between data points (0.5 nm) and the factor of c/λ^2 and summing all the data values.

$$\int \sigma^*(\lambda)\frac{c}{\lambda^2}d\lambda \approx \sum \sigma^*_{se}(\lambda_i)\frac{c}{\lambda_i^2}(0.5nm) = \frac{1}{X}\frac{e^2}{4mc\varepsilon_0}\left(f_{ed}+f_{md}\right) \tag{3.3-6}$$

The asterisk in the above equation indicates that this cross section is merely a curve with the correct shape, not the true cross section. The factor of X on the right-hand side of the equation is the as-yet undetermined scaling factor that must be multiplied by the cross section shape to obtain the correct magnitude. The table below outlines the process by which the measured fluorescence data was converted into the stimulate emission cross section. The integral mentioned in frame H was split into three parts for the neodymium-doped fiber to integrate each peak separately. The scale factor in frame I is calculated using the Judd-Ofelt method and the integral from frame H.

Stimulated Emission Cross Section								
A	B	C	D	E	F	G	H	I
Average Fluorescence	Calibration Function	(A-offset) x (B)	C x λ^5	D in regions where no SE	Linear fit of E for all points	D - F	Integral of G	G x (scale factor)

Table 6: An illustration of the data analysis methods used to calculate the stimulated emission section.

The Judd-Ofelt parameters and reduced matrix elements of the tensor operator used in calculating the electric dipole oscillator strengths of the possible emission transitions are presented in the following tables.

Parameters Used: Erbium	Value	Source
Excited State Lifetime	10.8 ms	Miniscalco, 1991
Refractive Index	1.462	Dragic & Papen, 1999
Judd-Ofelt 2	8.15 x10^{-20} cm^2	Ning et al, 2005
Judd-Ofelt 4	1.43 x10^{-20} cm^2	Ning et al, 2005
Judd-Ofelt 6	1.22 x10^{-20} cm^2	Ning et al, 2005
$(U2)^2$	0.0195	Carnall et al, 1968 (1)
$(U4)^2$	0.1173	Carnall et al, 1968 (1)
$(U6)^2$	1.4316	Carnall et al, 1968 (1)
M.D. Oscillator Strength	3.08 x10^{-7}	Carnall et al, 1968 (2)

Table 7: The parameters used in the erbium Judd-Ofelt calculation for the emission at 1530 nm along with the sources of each value.

Parameters Used: Neodymium	Value	Source
Excited State Lifetime	0.405 ms	Dragic & Papen, 1999
Refractive Index	1.462	Dragic & Papen, 1999
Judd-Ofelt 2	6.0 x10^{-20} cm^2	Gschnieder et al, 1998
Judd-Ofelt 4	4.7 x10^{-20} cm^2	Gschnieder et al, 1998
Judd-Ofelt 6	4.1 x10^{-20} cm^2	Gschnieder et al, 1998
$(U2)^2$ for 900 emission	0	Carnall et al, 1977
$(U4)^2$ for 900 emission	0.2283	Carnall et al, 1977
$(U6)^2$ for 900 emission	0.0554	Carnall et al, 1977
$(U2)^2$ for 1064 emission	0	Carnall et al, 1977
$(U4)^2$ for 1064 emission	0.1423	Carnall et al, 1977
$(U6)^2$ for 1064 emission	0.4083	Carnall et al, 1977
$(U2)^2$ for 1340 emission	0	Carnall et al, 1977
$(U4)^2$ for 1340 emission	0	Carnall et al, 1977
$(U6)^2$ for 1340 emission	0.2093	Carnall et al, 1977

Table 8: The parameters used in the neodymium Judd-Ofelt calculations for the three emission transitions along with the sources of each value.

The stimulated emission and ground state absorption spectra, determined using the methods outlined above, can be used to extract the excited state absorption cross section from pump-probe measurements. Equation 3.3-7 illustrates the relationship between the ratio of the transmission through the pumped and un-pumped optical fiber, and the sum of the three cross sections.

$$\ln\left(\frac{I_f^p}{I_f^u}\right) = \left(\sigma_{gsa} + \sigma_{se} - \sigma_{esa}\right)\overline{N}_2 L \qquad (3.3\text{-}7)$$

The average excited state population can be estimated by measuring the pump power exiting the fiber, using the known absorption to calculate how much pump power is

coupled into the beginning of the fiber, and then using Equations 2.3-6 and 2.3-7 to calculate the excited state population at the beginning and end of the fiber.

$$N_2 = N\frac{W_p\tau_2}{W_p\tau_2 + 1} \quad \text{where} \quad W_p = \frac{\sigma_{gsa} I_p}{h\upsilon_p}$$

The above equations, the measured pump power exiting the fiber, and an absorption cross section of 3.745 x10^{-21} cm^2 at 532 nm were used to estimate the excited ion fraction at both ends of the neodymium-doped fiber. At the end of the fiber, only 0.314% of the ions were estimated to be excited, while at the beginning of the fiber, 60.6% of the ions were estimated to be excited. Since the estimated excited population fraction at the beginning of the fiber is significant (more than 10%), the variation of the pump intensity with respect to position will no be purely exponential, and the estimation of initial pump power will be inaccurate. For our data analysis, then, the ground state absorption and stimulated emission cross sections will be scaled graphically.

Looking again at Equation 3.3-7, it is clear that when the spontaneous emission and ground state cross sections are removed, only negative values should remain. Additionally, it is useful that in erbium, there is no predicted excited state absorption or emission at the ground state absorption peak at 980 nm, and the cross section can be scaled directly from this peak. For neodymium, the well-known emission peak near 1060 nm will be used to determine the scale factor. Once the scaling factor is known, and the emission and ground state absorption cross sections have been subtracted, only the negative excited state absorption cross section remains. The table below demonstrates the data manipulation process.

Excited State Absorption Cross Section						
A	B	C	D	E	F	G
Average Pumped	Average Un-pumped	(A-offset) / (B-offset)	ln(C)	D / (Scale Factor)	E - σ_{gsa} - σ_{se}	-1 x F

Table 9: An illustration of the data analysis methods used to calculate the excited state absorption cross section.

4. Data Analysis

4.1 Reference Data

The tungsten bulb spectrum was measured to use a reference for future ground state absorption measurements, and to provide spectral calibration for the data collection apparatus.

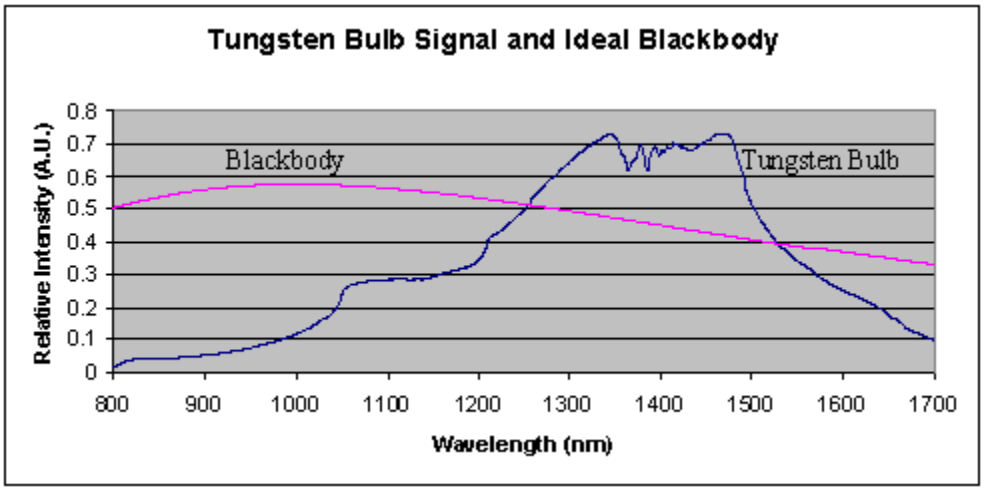

Figure 14: The measured tungsten bulb spectrum (higher curve) compared with the calculated blackbody radiation curve (lower curve) for a temperature of 2900 K.

In the above graph, the lower smooth curve represents the shape of the ideal blackbody spectrum for a temperature of 2900 K. This temperature was determined by Martin [2006] for the bulb used in this experiment. The magnitude of the curve was normalized to the central data point at 1250 nm.

The ideal blackbody radiation curve was divided, at each data point, by the measured tungsten bulb spectrum to obtain a calibration factor as a function of wavelength. Multiplying a measured signal by this calibration function would yield the true shape of that spectrum.

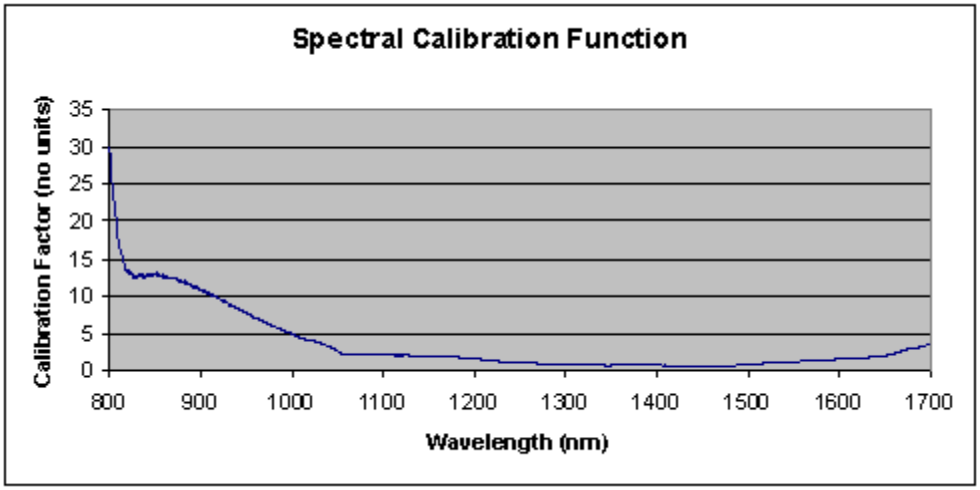

Figure 15: The spectral calibration of the data collection system calculated by dividing the ideal blackbody curve by the tungsten bulb signal.

The shape of the spectral calibration function, represented above, clearly demonstrates that the data collection system is optimized for infrared wavelengths in approximately the 1050 to 1650 nm range. The diffraction grating is blazed for 1500 nm, meaning it is most efficient at that wavelength, and the germanium photodetector is likewise most sensitive in this region. The sharp spike at 800 nm is no doubt due to the use of the 800 nm long-pass filter and the fact that the transmission of the filter is not a perfect step function at 800 nm. However, since the filter will be present in all measurements, there is no need to account for it independently.

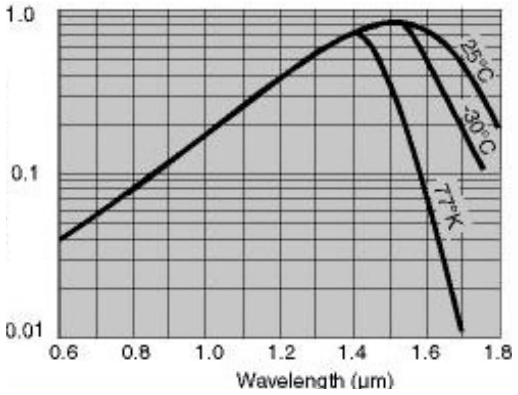

Figure 16: Responsivity of a Ge detector (dry ice = -78.5° C) as a function of wavelength [http://www.judsontechnologies.com/images/2.jpg].

Additionally, 1000 data points were collected with all light sources blocked to determine the systems electrical offset. These values were averaged to yield an offset of

0.0125 V. Regardless of the sensitivity of the lock-in, the values recorded on the computer are between 0 and 1 V, and the offset is the same. This electrical offset was subtracted from each data point that was measured using the data collection apparatus. These measurements include the tungsten bulb spectrum, the transmission through the doped fibers, the fluorescence of the doped fibers, and the pump-probe measurements.

4.2 Erbium Data

A data sheet did not accompany the erbium-doped fiber used in these experiments, so the numerical aperture, core diameter, and doping concentration were unknown. The doping concentration was later calculated by comparing the peak value of the absorption coefficient at 1530 nm measured in this experiment with that of previously measured erbium-doped silica fibers [Miniscalco, 1991]. The resulting concentration, as well as the other known fiber parameters, is listed in the table below.

Erbium Fiber		
Parameter	**Value**	**Source**
core diameter	Unknown	NA
length	160 cm	Measured
doping concentration	3.9×10^{18} cm^{-3}	Calculated
cut-off wavelength	Near 900 nm	Estimated
numerical aperture	Unknown	NA
excited state lifetime	10.8 ms	Miniscalco, 1991

Table 10: The erbium-doped fiber parameters.

The graph below represents the measured signal of the tungsten bulb light after passing through the erbium-doped silica fiber.

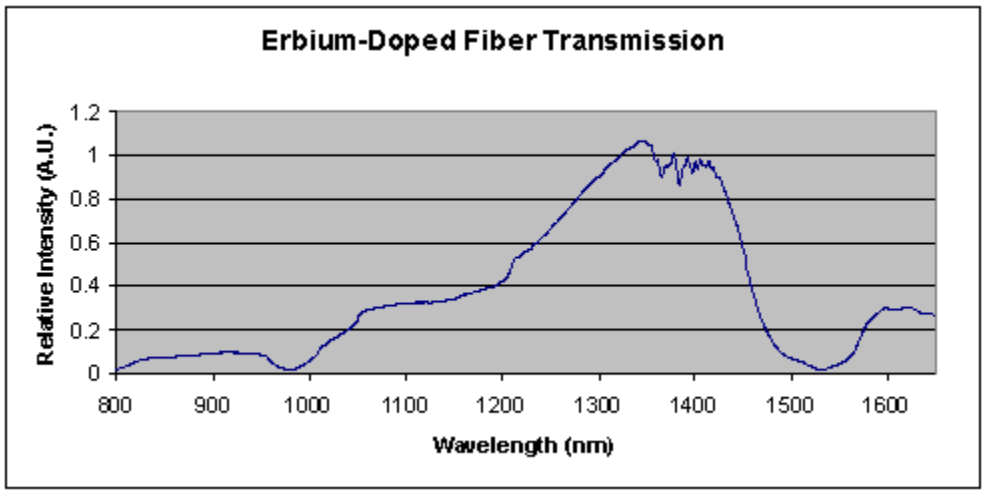

Figure 17: The six-scan average of the signal exiting the erbium-doped fiber.

There are two noticeable regions on the graph around 1000 nm and 1500 nm where there is evident absorption. Elsewhere, it closely resembles the shape of the measured tungsten bulb spectrum, the incident signal.

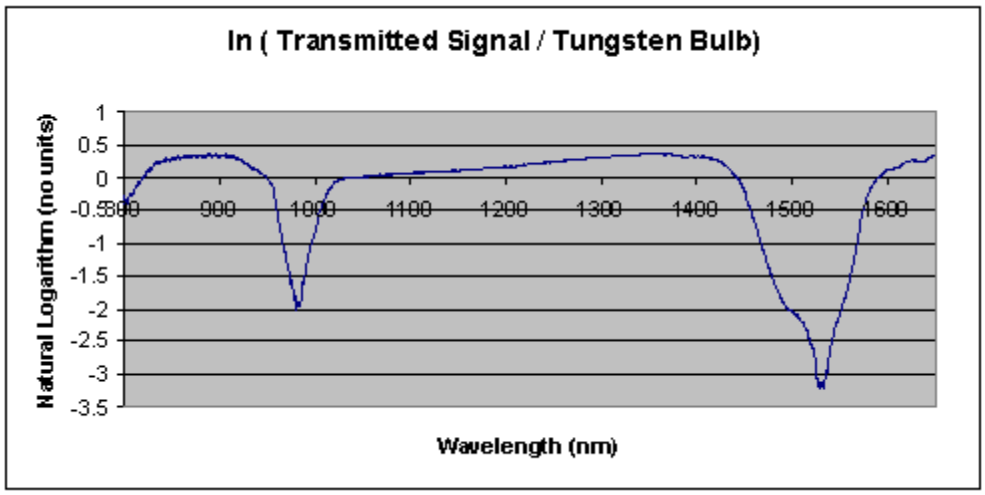

Figure 18: The natural logarithm of the average signal exiting the fiber divided by the tungsten bulb spectrum.

The two features mentioned above are clearly visible in the natural logarithm of the ratio between the transmitted signal and the tungsten bulb spectrum. In between these two regions, no additional ground state absorption is expected (see the Er energy structure diagram in Section 2.8). Based on the erbium energy diagram, there is ground state absorption at 800 nm, and the onset of that feature may be visible at the lower edge of the

scan range. The other changes in the data, such as the slope up between 1100 and 1400 nm, are partially the result of the index of the glass varying slowly with wavelength. By extrapolating the data points that are not part of the features seen at 800, 1000 and 1500 nm, and subtracting that contribution, only the erbium spectrum will remain.

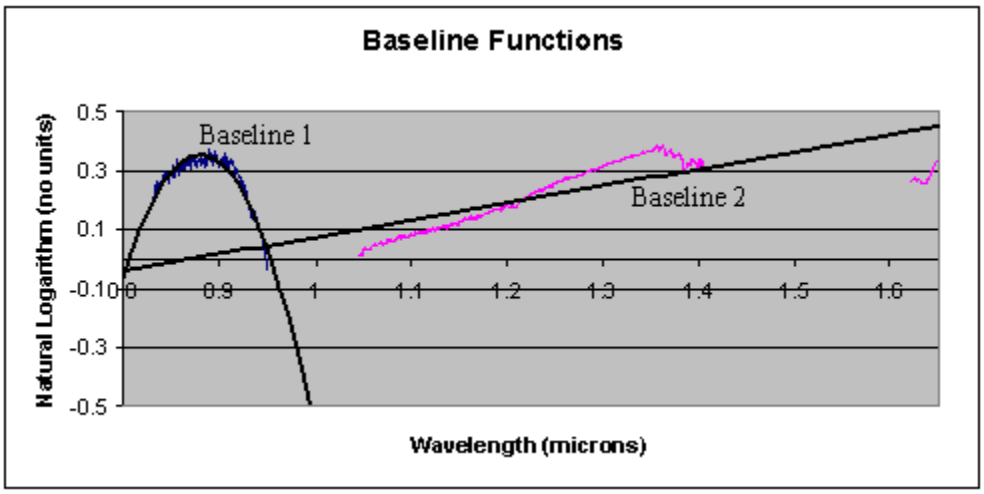

Figure 19: Two trend-lines were used to fit the data points that were in regions where no Er GSA was expected.

Two baseline functions were used because the cut-off wavelength of this fiber is believed to be between 900 and 1000 nm, however its effect is difficult to observe due to the Er absorption in this region. The quadratic baseline function was used for wavelengths less than 0.95 μm, or 950 nm, where the functions intersect. For longer wavelengths, the linear function was used. This combination of functions was subtracted for the natural log data, and the result was multiplied by negative one since the cross section must be a positive quantity.

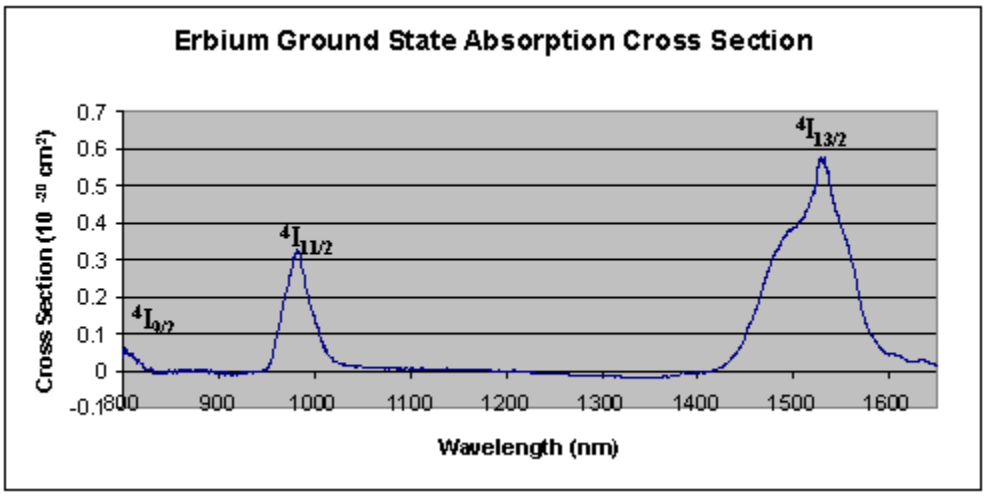

Figure 20: The ground state absorption cross section of Er in the silica fiber. The values used for the length and doping concentration of the fiber are listed in the table at the beginning of this section.

The two visible peaks in the above figure, along with the absorption edge near 800 nm, are labeled with the energy state to which the electron is excited when a photon is absorbed. The convention of labeling cross section peaks with the final state of the transition will be observed throughout the remainder of this report. The peaks of the two features entirely visible on the graph are at 984 and 1534 nm. These values are both within 4 nm of the peaks predicted by the energy diagram in Section 2.8. As can be seen from the figure, the transition at 1534 is significantly stronger than at 984 nm. When both measured peaks were integrated, the ratio of the oscillator strengths was found to be 1.8. Using the Judd-Ofelt procedure, the ratio of oscillator strengths was calculated to be 2.3, even larger than was observed. These values are at the edge of the 20% uncertainty inherent in the Judd-Ofelt method. Since not much is known about the exact composition of the host fiber, it is possible that the Judd-Ofelt parameters used were not the most ideal. The following reduced matrix elements were used in this calculation [Carnall et al, 1968 (1)]:

Wavelength	$(U2)^2$	$(U4)^2$	$(U6)^2$	f_{md}
1530	0.0195	0.1173	1.4316	3.08×10^{-7}
980	0.0282	0.0003	0.3953	0

Table 11: The squares of the three reduced matrix elements of the tensor operator and the magnetic dipole oscillator strength for the erbium GSA transitions.

The emission of the erbium-doped fiber was measured over the entire wavelength range, however only at wavelengths greater than 1350 nm was any non-zero signal observed.

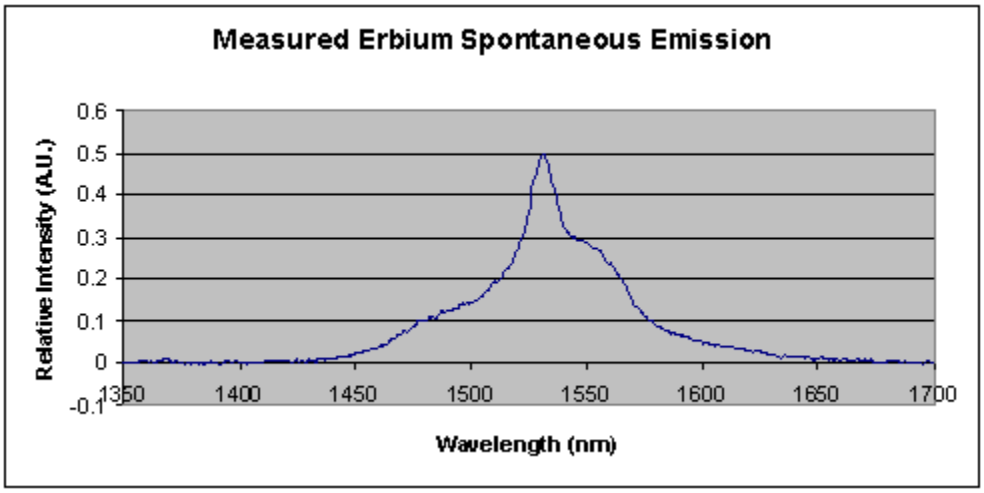

Figure 21: The average measured signal of the spontaneous emission perpendicular to the axis of the Er-doped fiber.

This data was then calibrated by multiplying by the spectral calibration function that was obtained by dividing an ideal blackbody spectrum at 2900 K by the tungsten bulb data.

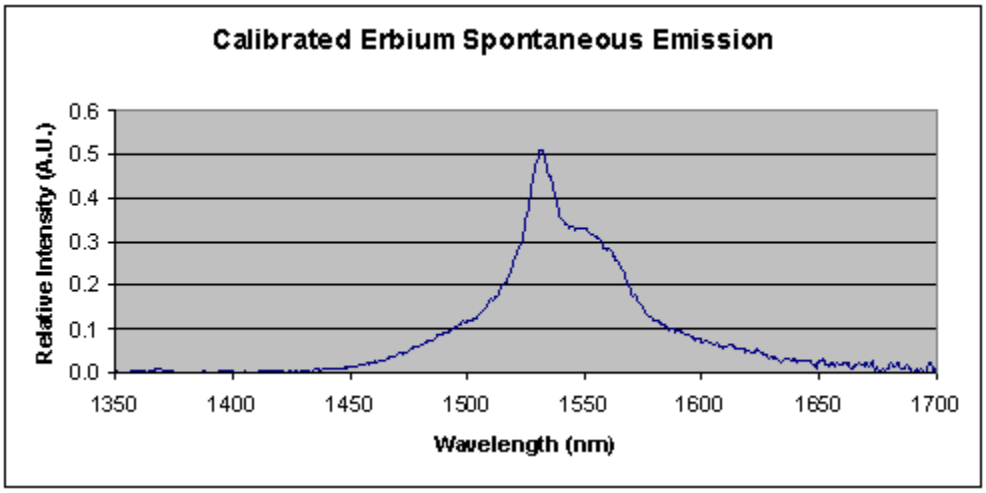

Figure 22: The corrected spectral shape of the spontaneous emission power per Δλ perpendicular to the axis of the fiber.

The flat regions at the edges of the graph should be very close to zero as the emission curve tapers down. However, since the calibration function is larger at between 1650 and 1700 than it is around 1400 nm, the slight zero offset that was not completely eliminated

is magnified. Besides this difference, the calibration function does not change rapidly over this wavelength region and the calibrated spectrum is very similar to the measured data.

The calibrated spontaneous emission spectrum was then converted into a curve with the same spectral shape as the stimulated emission cross section. Assuming no significant change in the index of refraction over this wavelength interval, the spontaneous emission spectrum was multiplied by a factor of λ^5. A baseline was matched to the regions to the left and right of the peak in the previous figure, so that the offset would not grow even larger when multiplied by the λ^5 factor. The resulting curve was integrated and the value of the integral was compared to the calculated integral using the Judd-Ofelt method. By dividing the theoretical value by the measured value, a scale factor was obtained and multiplied by the experimentally obtained curve. Since the data already had the correct spectral shape, the magnitude of each point was corrected to yield the true cross section.

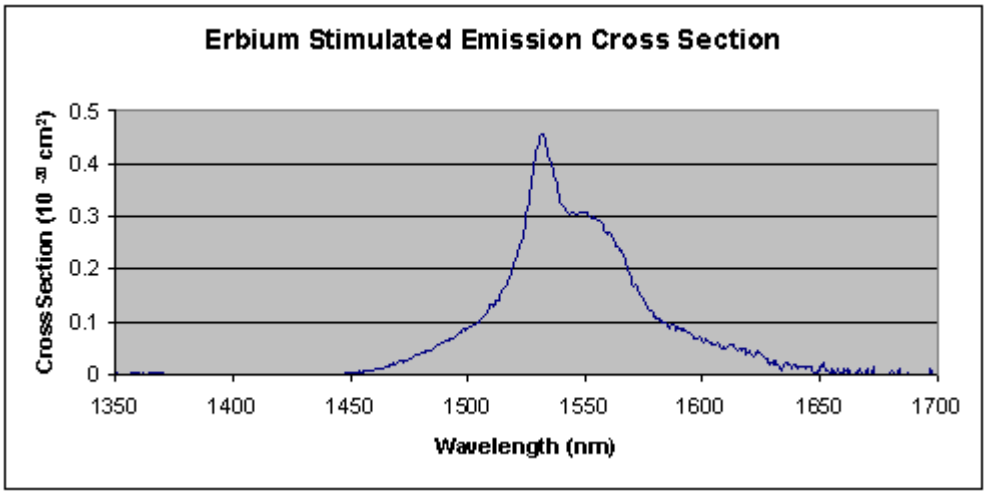

Figure 23: The stimulated emission cross section of Er in the silica fiber.

This stimulated emission cross section is of the same order of magnitude as the ground state absorption cross section, and is roughly 25% larger at the peak than the absorption at the same wavelength. This agrees well with previously measured stimulated emission spectra of erbium in silica glass fibers.

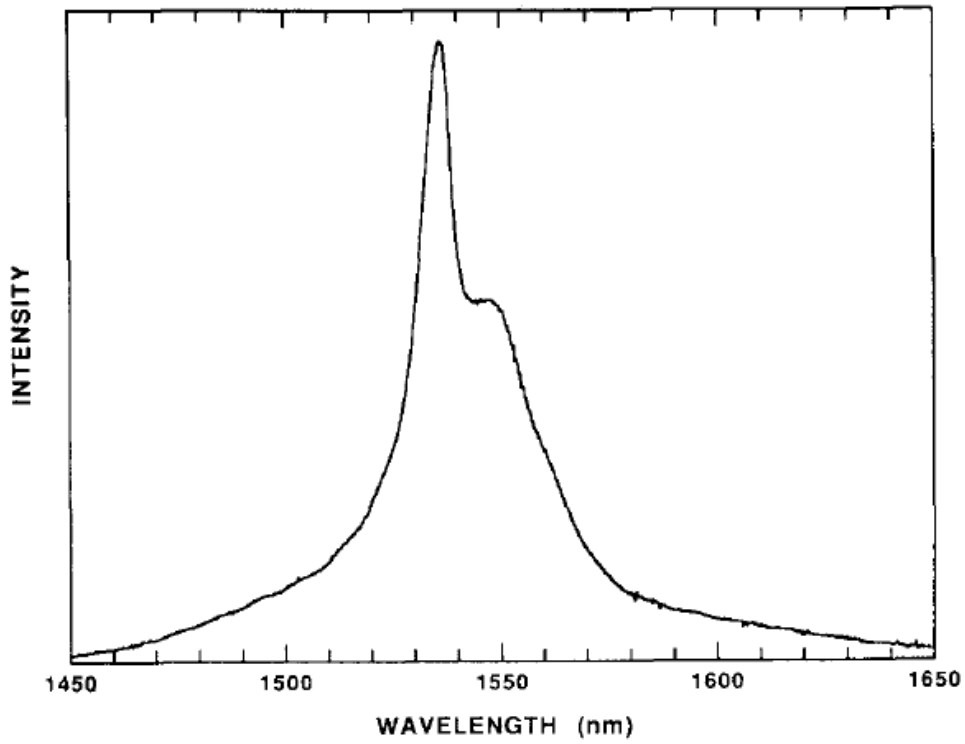

Figure 24: The stimulated emission spectrum of erbium in a silica glass fiber [Miniscalco, 1991].

Both the peak wavelength value and the shoulder from the spectrum measured in this thesis coincide with the wavelengths of the same features in the figure above, and is within 20% of the magnitude at the peak, as measured by Miniscalco [1991]. This indicates that the Judd-Ofelt method used to calculate the stimulated emission cross section from fluorescence is effective within its margin of error.

Once the ground state absorption and stimulated emission cross sections have been obtained, it is possible to use them to determine the excited state absorption cross section from pump probe measurements. A beam splitter was used to couple both a portion of the laser pump power and the tungsten bulb signal into the Er-doped fiber. Measurements were then taken with the pump on, and with the pump off. Besides the blocking of the pump laser, no other change was made to the experimental set-up between pumped and un-pumped measurements.

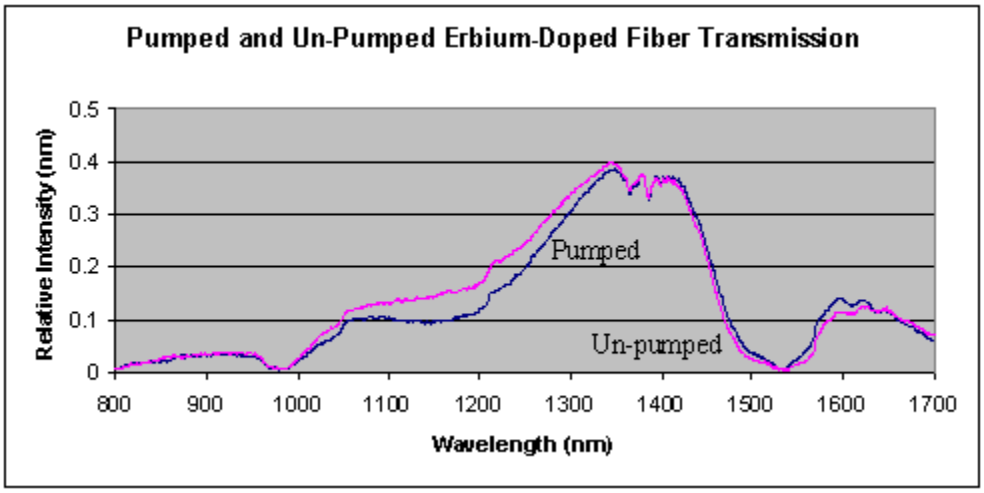

Figure 25: The measured signals exiting the fiber in the pumped (blue) and un-pumped (pink) cases.

Between roughly 1000 and 1350 nm, there is a clear difference between the two signals, with the un-pumped signal being the larger of the two. In the 1500 to 1600 nm range, while the difference is not as evident due to the lower signal strength, the pumped signal is larger. By taking the natural log of the ratio of the pumped and un-pumped signals, the differences become more pronounced.

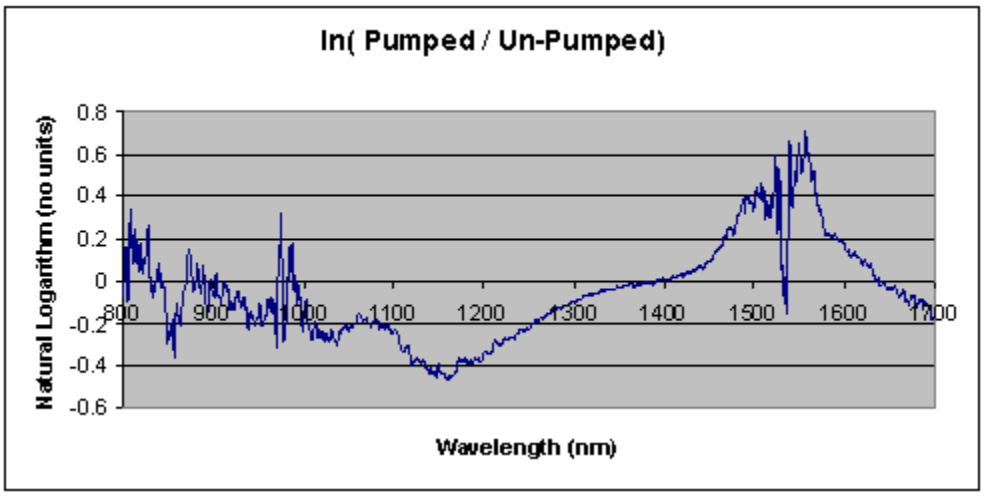

Figure 26: The natural logarithm of the ratio of the pumped and un-pumped signals.

This quantity is proportional to the sum of the ground state absorption and stimulated emission cross sections minus the excited state absorption cross section. The constant of proportionality is the average excited state population density multiplied by the path

length. Most unexpected is the very sharp drop at 1535 nm, when no excited state absorption is predicted in this region. One possible explanation for this is the phenomenon known as 'site selection'. Glass is a non-uniform host, and therefore it is possible for the dopant erbium ions to be exposed to a variety of different nearest-neighbor atom configurations. Each configuration would have a slightly different effect on the Er ion's Hamiltonian due to the crystal field effect. As discussed in Section 2.8, the pump wavelength of 532 nm does not coincide with an absorption peak for Er, but rather is on the edge of a peak. The site selection hypothesis suggests that the ions whose crystal field enables them to absorb the off-peak pump wavelength will not be the ions absorbing strongly at the ground state absorption peak at 1534 nm. If this is true very little, if any, bleaching will be observed. Since there is strong absorption at this wavelength, both signals become very small and nearly equal. The ratio of the two signals is unity at this point, and thus the natural log drops to zero.

There is zero excited state absorption expected at 980 nm and no emission, and therefore the peak seen there is due entirely to bleaching of the ground state absorption. Bleaching is the term used to describe the increased signal in the pumped case that is due to fewer absorbing ions in the ground state. The ground state absorption spectrum was then plotted with the data shown above. An adjustable scaling factor was used to fit the ground state absorption cross section to the pump-probe data at 980 nm.

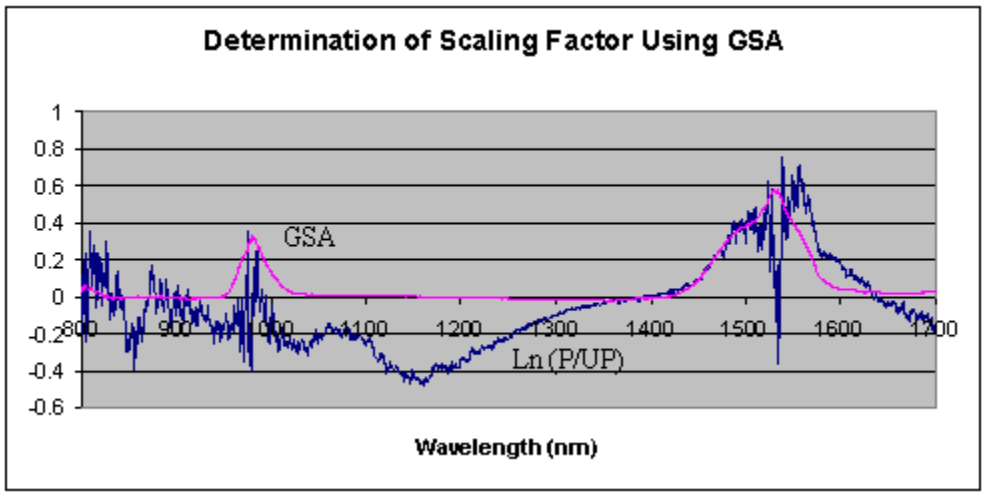

Figure 27: The ground state absorption cross section was scaled graphically to match the peak value at 980 nm

Fitting the data in this manner yielded a scaling factor of 1.0 $x10^{20}$. After dividing by the fiber length, 160 cm, the average excited state population density was calculated to be 6.3 $x10^{17}$ cm^{-3}. This is equivalent to a excited fraction of 0.16. After subtracting the scaled ground state absorption, the stimulated emission cross section was compared to the remaining data.

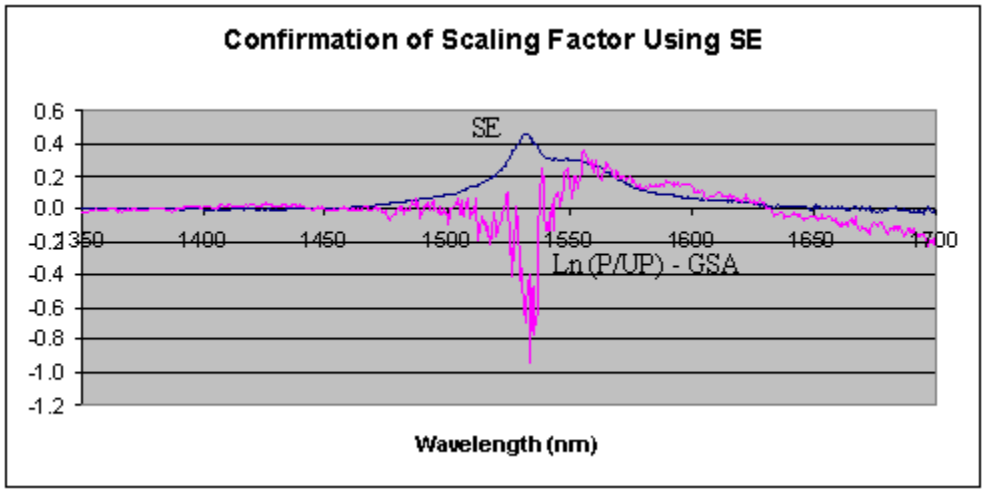

Figure 28: The stimulated emission cross section was compared to the log data after subtracting the GSA cross section. The same scale factor was used.

Using the same scaling factor as the ground state absorption cross section, the stimulated emission cross section accounted for all the remaining positive data. This indicates that the scaling of the stimulated emission cross section done using the Judd-Ofelt method was accurate to within the predicted 10-20% uncertainty.

Finally, the log of the pumped/un-pumped ratio was scaled using the factor determined graphically and the GSA and SE cross sections were subtracted. The result was multiplied by negative one to yield the excited state absorption cross section.

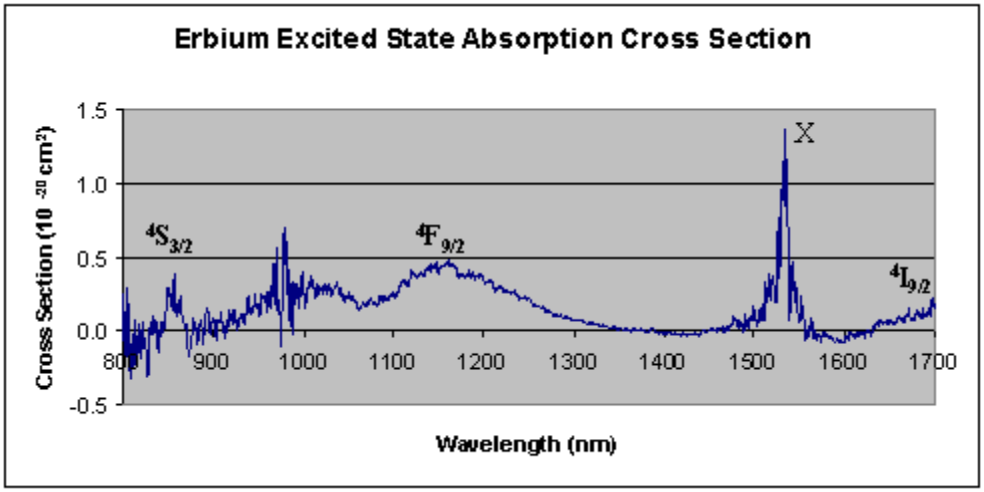

Figure 29: The excited state absorption cross section of erbium in the silica fiber.

Three features, predicted by the erbium energy level diagram, are labeled with the excited energy state to which an electron would be excited. The excitation to the $^4I_{9/2}$ state is predicted to occur at 1680 nm, however appears to be shifted past 1700 nm off the edge of the graph. The peak labeled 'X' is entirely unexpected, but could be explained by the previously discussed site selection hypothesis. The noise at 980 nm is due to the ground state absorption at that wavelength being large enough to make both signals small. When dividing two low signals, small deviations become more critical. Unexplained, however, is the apparent peak slightly past 1000 nm where there are no expected transitions. Both signals are quite small in this region and the size of the ratio of the two would vary considerably with the averaged electrical offset. If the offset value were too large, the ratio would be magnified in the small-signal region and what is really the slope up to the peak 1150 nm could appear as it does on the graph above.

The purpose of these measurements was to determine if an excited state absorption cross section could be measured using the pump-probe technique and the equipment available in the lab. Two definite peaks were observed, as well as the onset of an expected transition at the edge of the scan range. With the exception of the noise at 980 nm, there was a favorable signal-to-noise ratio. The same measurement procedures will therefore be repeated for the neodymium-doped silica glass fiber.

4.3 Neodymium Data

A 2-meter segment of neodymium-doped silica fiber was used for the measurements discussed below. The Nd doping concentration was approximately 600 ppm by weight, but without knowing the density of the fiber, the ion per unit volume density could not be accurately determined. This parameter was therefore calculated in the same manner as it was for the erbium-doped fiber. This fiber is also co-doped with tantalum and was fabricated using an aerosol deposition technique at Boston University. The ground state absorption of the fiber was measured, and an absorption peak was compared to a previously measured absorption cross section of Nd in silica glass [Martin, 2006]. The parameters used for the Nd-doped fiber are displayed in the table below.

Neodymium Fiber		
Parameter	**Value**	**Source**
Core diameter	5 μm	Fiber data sheet
Length	204 cm	Measured
Doping concentration	8.1×10^{17} cm^{-3}	Calculated
Cut-off wavelength	740 nm	Fiber data sheet
Numerical aperture	0.12	Fiber data sheet
Excited state lifetime	405 μs	Dragic & Papen, 1999

Table 12: The neodymium doped fiber parameters.

The graph below is the average of six measurements of the tungsten bulb signal after passing through the neodymium-doped fiber. The scan parameters used for this measurement, and all of the following measurements, are displayed in tables in Section 3.2.

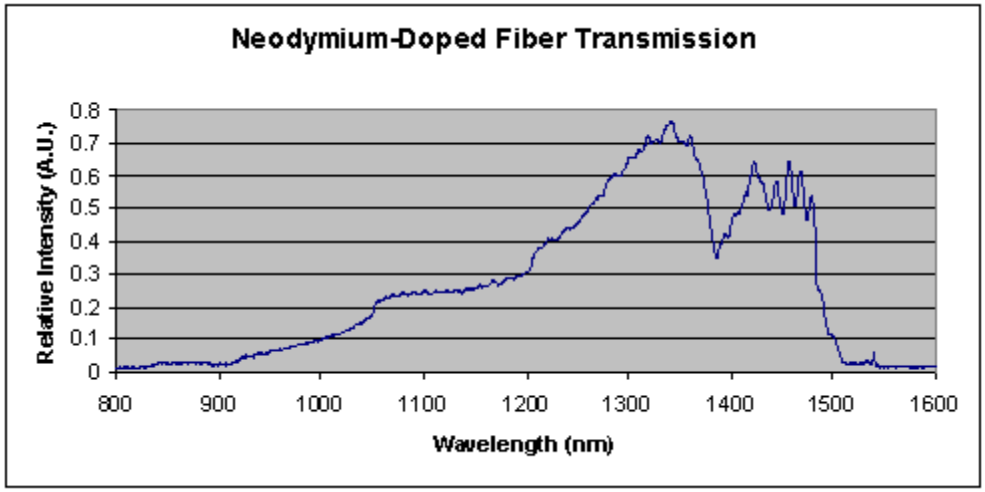

Figure 30: The measured light spectrum exiting the Nd-doped silica fiber.

This data resembles the spectral shape of the tungsten bulb spectrum in most regions, with three apparent exceptions. The signal strength at wavelengths shorter than 900 nm and longer than 1500 nm becomes very small. Additionally, there is an evident absorption peak at 1387 nm. There is no neodymium ground state absorption transition expected at this wavelength, so this is the result of OH^- ion absorption (see Section 2.11).

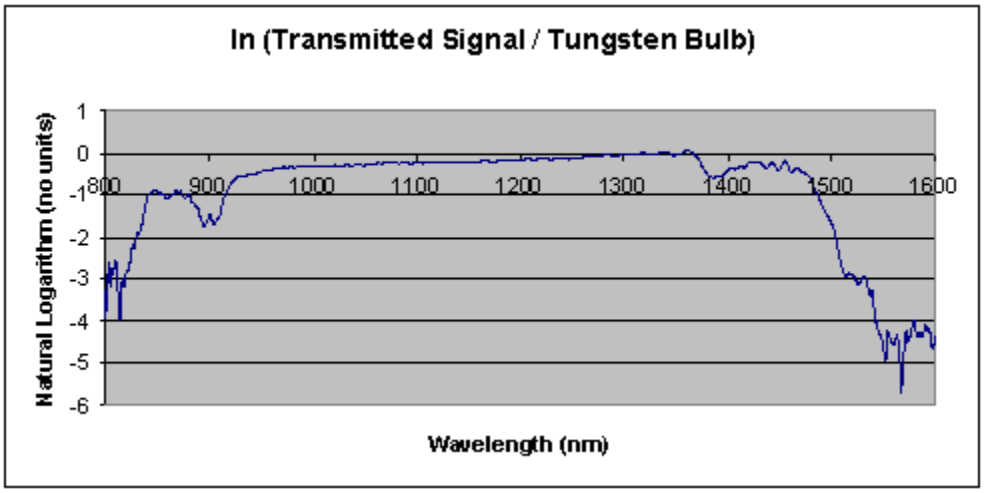

Figure 31: The natural logarithm of the measured light exiting the fiber divided by the tungsten bulb spectrum.

After taking the natural logarithm of the ratio of the light transmitted through the fiber to the tungsten bulb spectrum, these absorption features become easier to identify. While the OH^- ion absorption appeared large in the previous figure, in the graph above it is revealed to be small, less than half at the peak, compared to the other absorption peaks. A trend-

line was fit to the data not incorporated into one of these features to compensate for reflection and other effects. The OH^- ion absorption was also subtracted because it will not play a role in the pump-probe measurements. The neodymium ground state absorption will be affected by bleaching, but the OH^- ion absorption will not and will therefore cancel out.

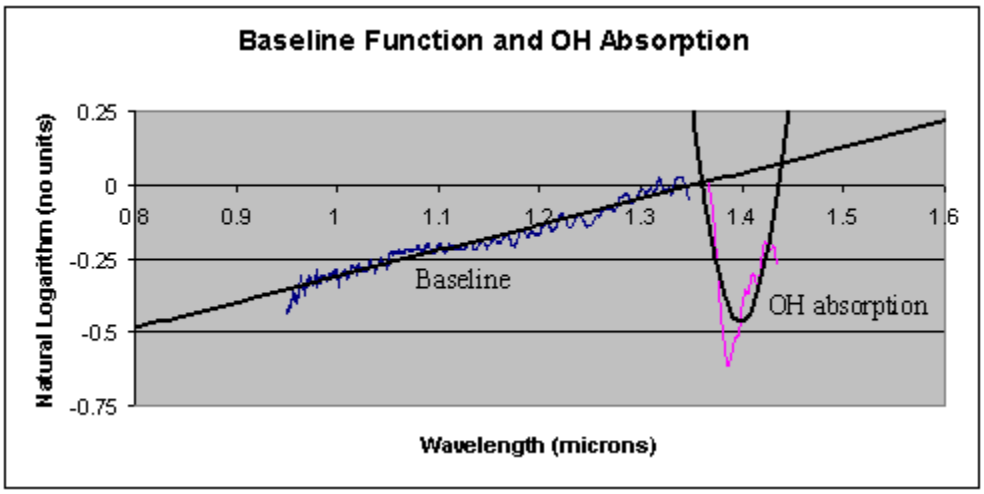

Figure 32: A baseline was used to fit the data between the absorption features (linear) and another was used to remove the OH contribution (parabolic).

The linear data, representing the baseline function, was subtracted from all points of the spectrum. The parabolic curve, used to approximately fit the OH^- ion absorption, was subtracted only from wavelengths for which the function is negative. This effectively removes the OH^- ion absorption peak from the ground state absorption spectrum of Nd. Once the baseline and OH^- ion absorption curves were subtracted, the resulting data was multiplied by negative one and divided by the length of the fiber. The peak value of the absorption coefficient at 900 nm obtained from this procedure was compared to the cross section previously determined by Martin [2006]. The Nd ion number density, seen in the table at the beginning of this section, was calculated by this method for the sample fiber. The measured absorption coefficient was then divided by this Nd ion number density in order to obtain the cross section at other wavelengths.

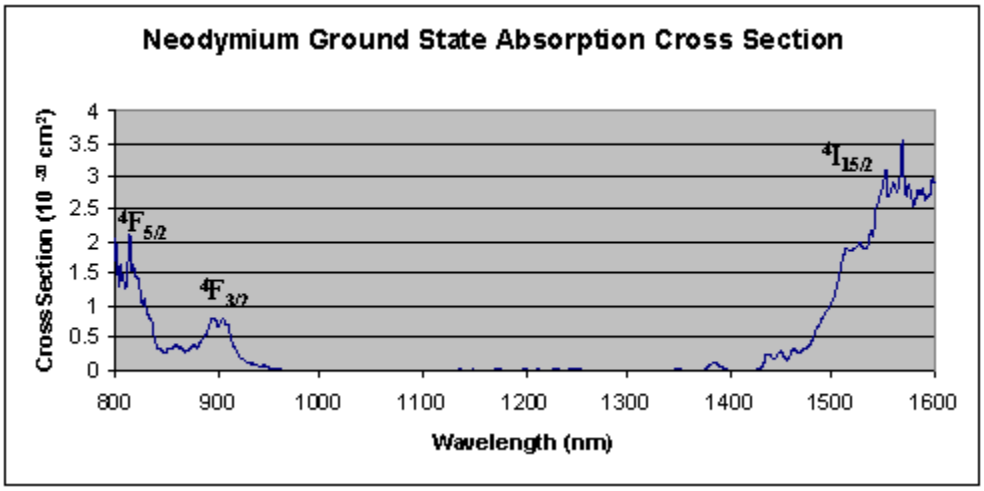

Figure 33: The ground state absorption cross section of Nd in the silica fiber.

Based upon the neodymium energy level diagram in Section 2.2, no absorption was expected between 1000 and 1400 nm. The ground state absorption spectrum shown in Figure 33 is consistent with this, and shows the entire $^4F_{3/2}$ transition, but only the lower and upper edges of the $^4F_{5/2}$ and $^4I_{15/2}$ transitions. The noise at the peaks on either end of the spectrum is most likely due to the very small signal in those regions.

The spontaneous emission of the pumped neodymium-doped fiber was measured perpendicular to axis of the fiber. The average of six measurements is presented in the figure below.

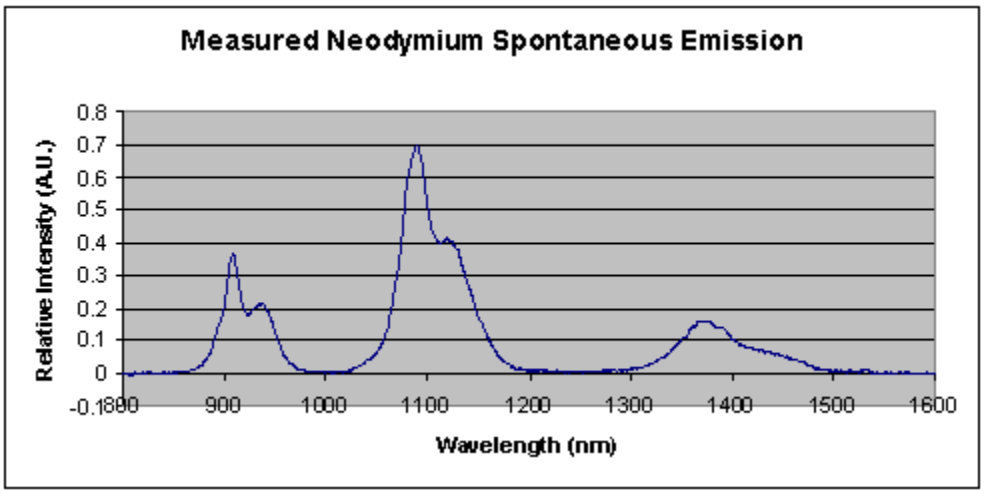

Figure 34: The measured spontaneous emission from the Nd-doped silica fiber pumped at 532 nm.

This measured data was then multiplied by the spectral calibration function to reveal the true spectral shape of the spontaneous emission.

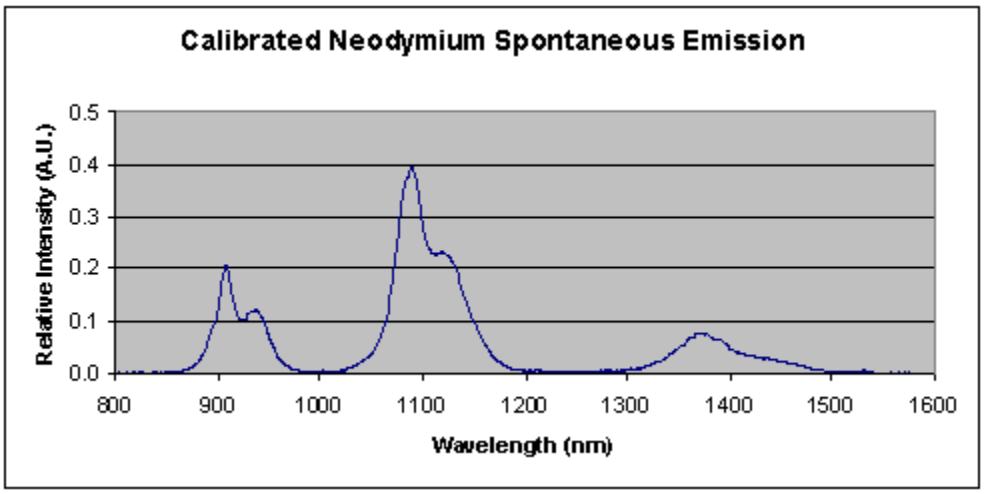

Figure 35: The calibrated spontaneous emission power per Δλ, adjusted to compensate for the non-uniform detector/diffraction grating efficiency.

Most notable about the spectrum displayed in Figure 35 is the lack of a strong emission peak at 1064 nm. The peak at 1340 nm is missing as well. It is very unusual for these Nd transition to be shifted 30 nm to longer wavelengths. One possible hypothesis is that there is fluorescence quenching by the hydroxyl ions present in the glass. An excited neodymium ion would transfer energy to a neighboring OH ion, by which the OH ion is excited and the Nd ion is reduced to one of its lower energy states. The two ions then both decay via non-radiative means to the ground state. This has the effect of reducing the excited state lifetime of the Nd ions. It has been proposed that there is a possible correlation between OH and Nd sites [Ehrmann et al, 2004]. If this is true, a phenomenon similar to site selection, discussed in the Erbium Data section, could be taking place. Neodymium ions that would normally emit at 1064 nm are being quenched, while off-peak ions with a different crystal field effect are not. This would account for why the strongest emission is not measured at 1064 nm, however it is difficult to imagine that the fluorescence quenching is severe enough that no peak or inflection point is observed at that wavelength. In addition, the samples used in Ehrmann's study that demonstrated significant quenching had an OH concentration of 900 ppm, as compared to the Nd-doped fiber used in this thesis with an OH concentration of 57 ppm. Therefore, unless this particular silica glass host causes strong pairing between OH and Nd ions, the

quenching phenomenon is likely too small to be entirely responsible for the lack of a peak at 1064 nm.

The McCumber relation, described in Section 2.6, was used to convert the calibrated spontaneous emission into a curve with the same spectral shape as the stimulated emission cross section. Again assuming that the index of refraction did not vary significantly with wavelength, each data point was multiplied by a factor of λ^5. Since this caused any slight electrical offset, not compensated for by the average value of 0.01245 subtracted from all measurements, to become noticeably larger, a baseline was fit to the points between emission peaks. This yielded a curve that was proportional to the stimulated emission cross section. The integral over each of the three separate peaks was calculated in order to obtain the proportionality constant. Each of these three integrals was compared to the theoretical value calculated using the Judd-Ofelt method. Three scale factors were obtained in this manner, and the average of the three was used to scale the stimulated emission cross section. The calculation used to determine the scale factor is displayed in the table below.

Stimulated Emission								
Emission to State	Wavelength	$(U2)^2$	$(U4)^2$	$(U6)^2$	f	Calculated Integral	Measured Integral	Scale Factor
$^4I_{9/2}$	900	0	0.2283	0.0554	5.1×10^{-6}	3.4×10^{-12}	5.0×10^{11}	6.9×10^{-24}
$^4I_{11/2}$	1064	0	0.1423	0.4083	7.8×10^{-6}	5.2×10^{-12}	9.2×10^{12}	5.7×10^{-25}
$^4I_{13/2}$	1340	0	0	0.2093	2.3×10^{-6}	1.5×10^{-12}	1.8×10^{12}	8.6×10^{-25}
							Average:	2.8×10^{-24}

Table 13: The calculated and measured cross section integrals for the three neodymium emission transitions.

Multiplying the calibrated spontaneous emission spectrum by λ^5 and the average scale factor yielded the stimulated emission cross section.

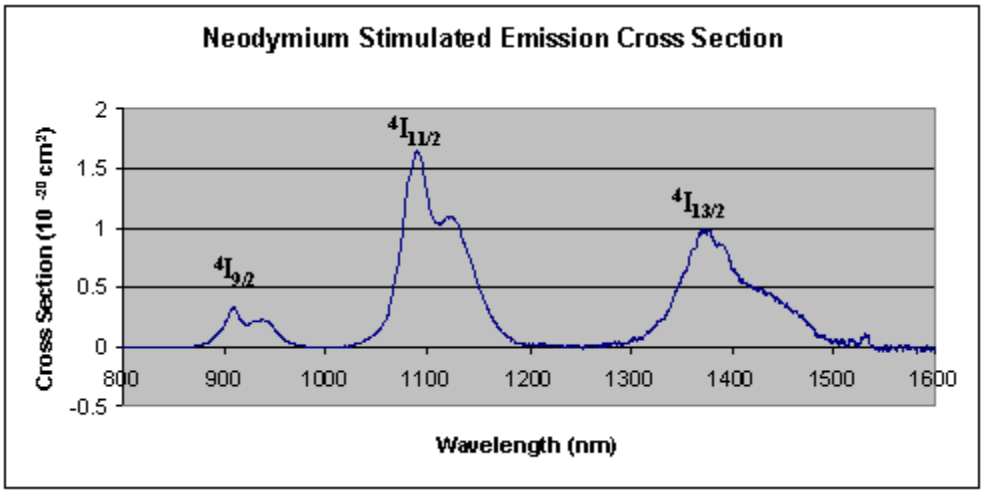

Figure 36: The stimulated emission cross section of Nd in the silica fiber.

The peak height of the $^4I_{11/2}$ transition, at 1092 nm, is close to the predicted peak cross section in high silica glass of 1.5 x10^{-20} cm^2 [Stokowski et al, 1981]. According to the theoretically calculated oscillator strengths, the integral of the peak at 900 nm should be larger than that of the peak at 1400 nm. The index of refraction over the scan range was assumed to be constant since it changes very slowly. In general, the index of refraction is larger at smaller wavelengths. Therefore, including this effect, if noticeable, would only have exacerbated the disparity in peak height. The cause of the difference from the expected results is unknown.

The pump-probe measurements were then conducted by coupling the 532 nm pump laser light and the tungsten bulb light into the doped fiber via a beam splitter. The transmitted light was measured when the pump light was present, and again when the pump laser was blocked. Besides the blocking/un-blocking of the laser, no other change was made to the experimental configuration between scans.

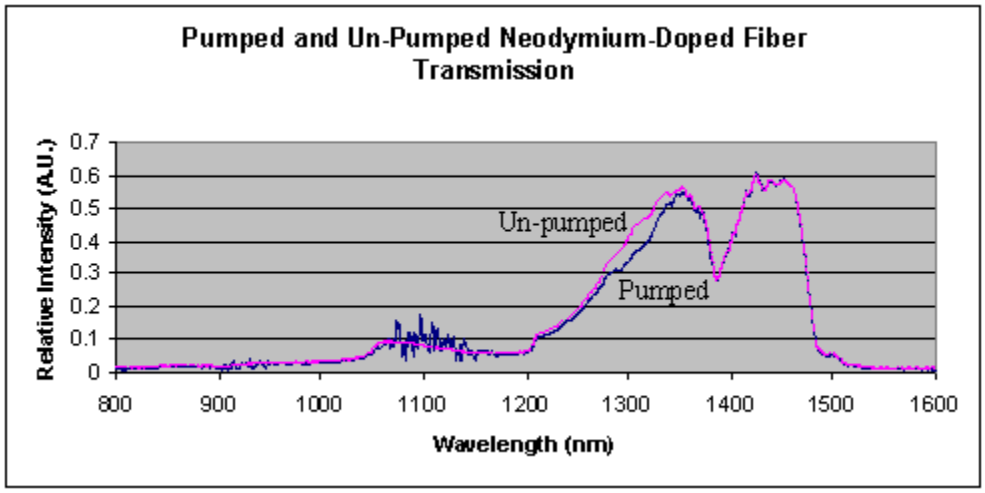

Figure 37: Tungsten bulb light transmitted through the pumped (blue) and un-pumped (pink) silica fiber.

The most identifiable discrepancy between the pumped and un-pumped measurements occurs at approximately 1300 nm. Since the magnitude of the un-pumped signal is larger in this region, it is evidence of excited state absorption. Surprisingly, a clear gain signal at 1092 nm was not observed, as this portion of the data was exceedingly noisy. This could be due in part to fluctuations of the spontaneously emitted light. Examining the signal in this region on the oscilloscope indicated that these were low frequency fluctuations of a significantly greater magnitude than the bulb signal. Taking the natural logarithm of the pumped divided by the un-pumped data reveals more details about the differences between the two signals.

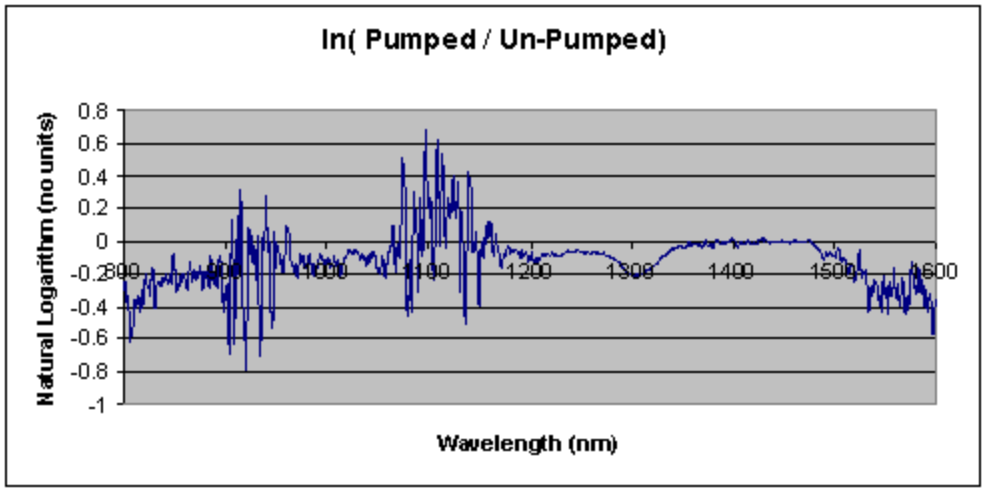

Figure 38: The natural log of the pumped signal divided by the un-pumped signal.

As seen in the graph above, there is a clear excited state absorption peak at 1300 nm. However the small gain expected from Figure 1 in the introduction is not present. From this data, it is possible to see gain at the 1092 nm wavelength, however the exact magnitude is difficult to determine due to the noise. There is also significant noise near the 900 nm spontaneous emission peak, likely due to the same cause as the noise at 1092 nm. The stimulated emission cross section, multiplied by an adjustable scaling parameter, will be compared with this data to determine the average excited state population density.

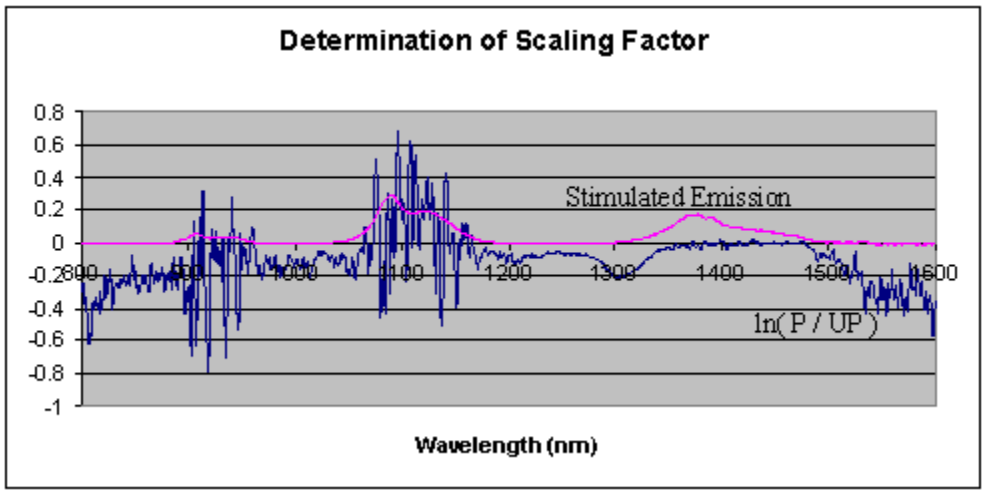

Figure 39: The natural log data seen in the previous figure graphed along with the stimulated emission cross section multiplied by a scale parameter.

The scaling parameter used to obtain this fit was 1.75 x10^{19}. Dividing this parameter by the length of the fiber, 204 cm, yields an average excited population number density of 8.6 x10^{16} cm^{-3}. This is equivalent to 10.6% ($\pm$ 2%) of the Nd ions in the fiber. In Section 3.3, estimates of the excited state population percentage at the beginning of the fiber, 60.6%, and at the end, 0.3%, were calculated. Assuming a purely exponential change over the length of the fiber, this would predict an average excited population of 11.4% ($\pm$ 2%). These two values are in agreement, well within the uncertainty.

The natural log of the pump probe data was divided by the scale factor, and the spontaneous emission and ground state absorption cross sections were subtracted. The resulting data was multiplied by negative one to obtain the excited state absorption cross section, and is shown below in Figure 40.

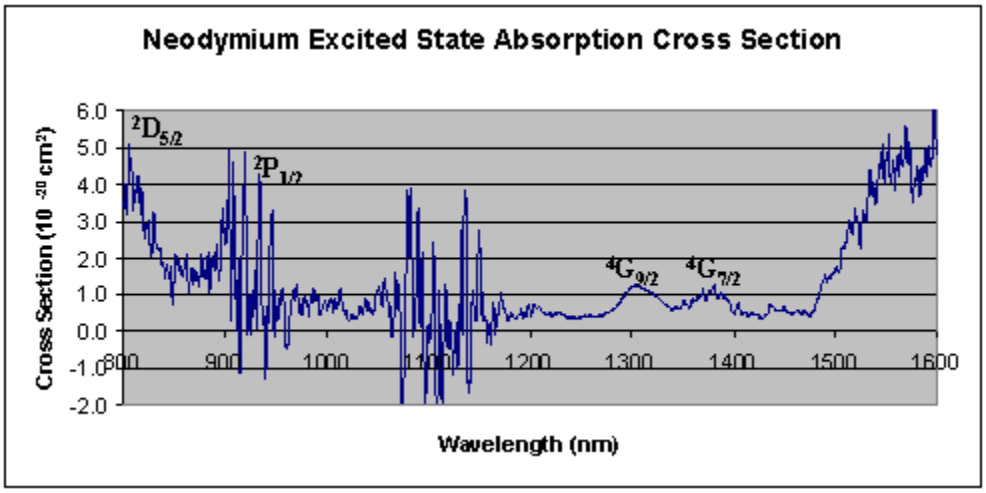

Figure 40: The excited state absorption cross section of Nd in the silica glass fiber.

The peaks that are readily identifiable from this graph are labeled with the final energy states of the transitions. The excited state absorption at 1300 is due to two close energy states, the $^4K_{13/2}$ and the $^4G_{9/2}$ states. The $^4G_{9/2}$ label was used on the graph since its oscillator strength is more than an order of magnitude larger. The oscillator strengths for the excited state absorption transitions within the wavelength range scanned for these experiments are calculated in the table below.

Excited State Absorption						
ESA To State	Wavelength	$(U2)^2$	$(U4)^2$	$(U6)^2$	f	Calculated Integral
$^2D_{5/2}$	800	0.0009	0.0007	0	3.8×10^{-8}	1.0×10^{-13}
$^2P_{1/2}$	840	0.0131	0	0	3.3×10^{-7}	8.8×10^{-13}
$^2K_{15/2}$	960	0	0	0.0076	1.1×10^{-7}	3.1×10^{-13}
$^4G_{11/2}$	960	0	0.0015	0.0992	1.5×10^{-6}	4.0×10^{-12}
$^2D_{3/2}$	1030	0.005	0	0	1.0×10^{-7}	2.8×10^{-13}
$^2K_{13/2}$	1200	0	0	0.0076	9.2×10^{-8}	2.5×10^{-13}
$^4G_{9/2}$	1200	0	0.057	0.1451	2.5×10^{-6}	6.8×10^{-12}
$^4G_{7/2}$	1300	0.1062	0.0629	0	2.5×10^{-6}	6.8×10^{-12}
$^4G_{7/2}$	1700	0.0735	0.04	0	1.3×10^{-6}	3.5×10^{-12}
$^4G_{5/2}$	1700	0.4856	0.0433	0	6.5×10^{-6}	1.7×10^{-12}

Table 14: The calculated oscillator strengths and cross section integrals for the Nd excited state absorption transitions.

The transition wavelengths listed in the table above are from the neodymium energy level diagram for a fluoride glass host given in Section 2.2, and have been, for the most part, shifted to longer wavelengths in the silica glass host used in this thesis. The pumped and un-pumped signals below 1000 nm were both very small and the size of their ratio would vary dramatically depending on the electrical offset. For wavelengths between 1200 and 1500, the focus of this investigation, the signal strength is large enough compared to the offset to be confident in the cross section magnitudes.

The ground state absorption, stimulated emission, and excited state absorption are all plotted on the same scale in the graph below.

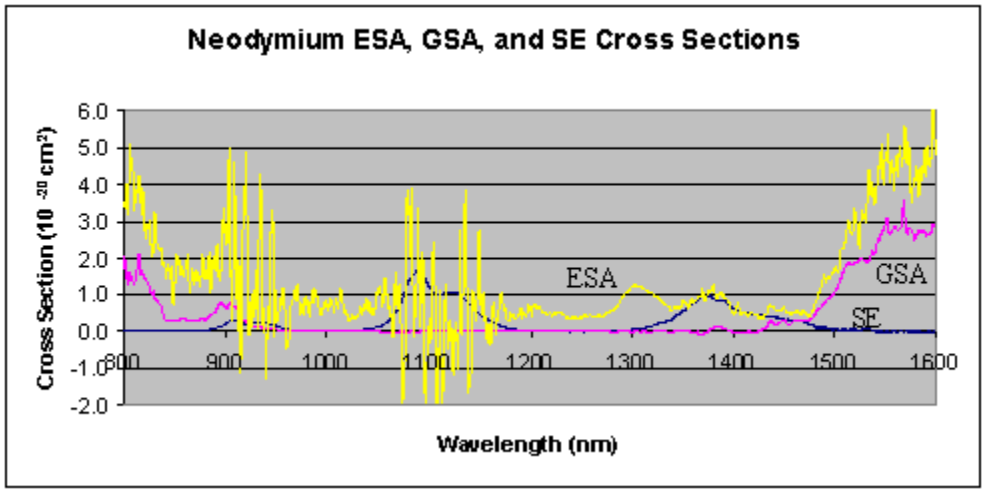

Figure 41: The excited state absorption (ESA), ground state absorption (GSA), and stimulated emission (SE) cross sections of Nd in silica glass fiber.

The excited state absorption cross section is large enough to negate the effects of the stimulated emission peak at 1380 nm and result in approximately zero net gain or loss between the wavelengths of 1370 and 1470 nm. The excited state absorption at both edges of the scan range is larger than the corresponding ground state absorption in the same area. Under the conditions of this experiment, the pumped signal was only noticeably larger than the un-pumped signal near the 1092 emission transition.

5. Conclusions

The results of the pump-probe experiment for the neodymium-doped silica fiber did not demonstrate noticeable gain from the $^4F_{3/2}$ to $^4I_{13/2}$ emission transition.

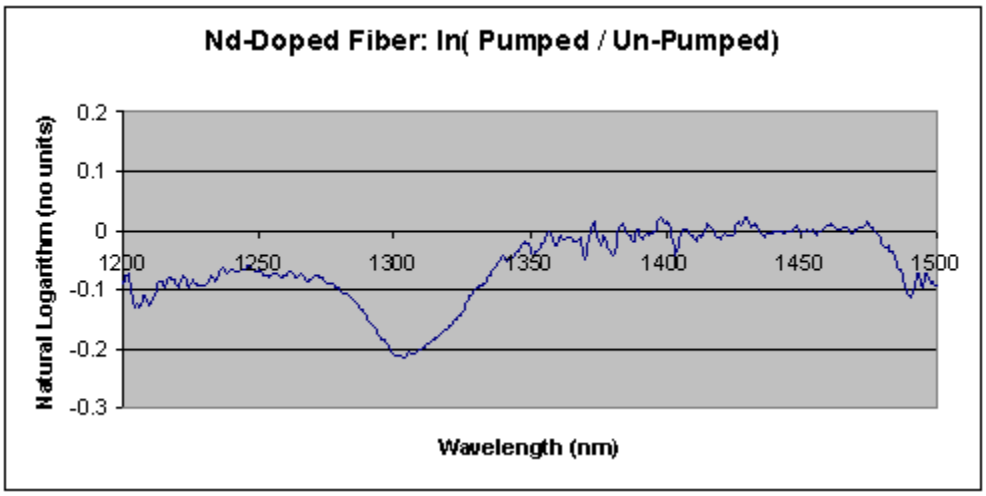

Figure 42: The natural log of the ratio of the transmitted light through the pumped and un-pumped Nd-doped fiber.

For the natural logarithm data above, positive values indicate that the signal from the pumped transition was larger and negative values indicate that the un-pumped signal was greater. There is definite absorption at 1300 nm due to the $^4G_{9/2}$ excited state absorption transition. The peak of the measured emission in this region was at 1380 nm, and while there is no loss at this wavelength, nor is there any observed gain beyond the noise. It appears that for the wavelengths between 1350 and 1475 nm, the stimulated emission and excited state absorption cross sections have effectively canceled one another. While the phenomenon that caused the absence of the 1064 and 1340 nm peaks is unknown, it has definitely affected the stimulated emission spectrum. It is therefore likely that the overall scaling of the emission spectrum could show more than the 20% uncertainty inherent in the Judd-Ofelt method.

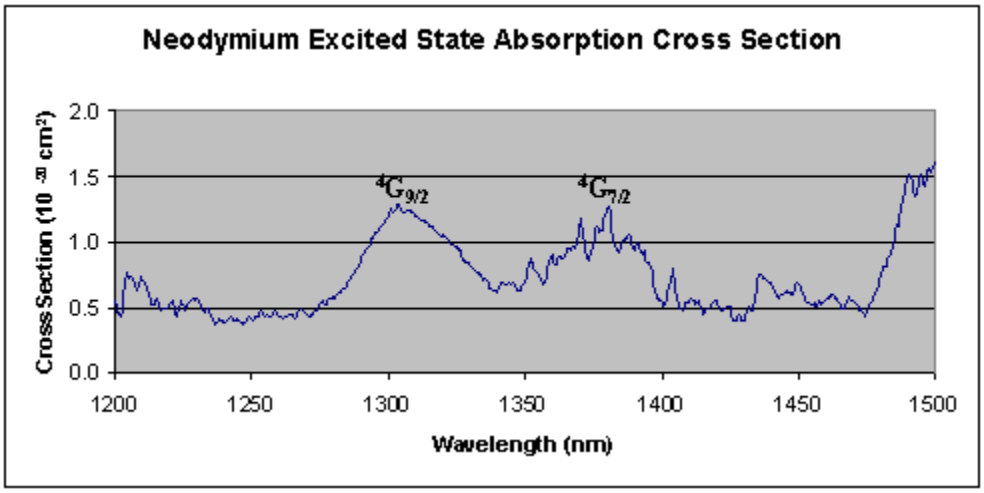

Figure 43: The excited state absorption cross section of Nd in the silica glass fiber over the 1200 to 1500 nm wavelength range.

The excited state absorption cross section shows two peaks, each of which have been shifted nearly 100 nm to longer wavelengths in the silica glass fiber than predicted by the energy structure of neodymium in a fluoride glass host.

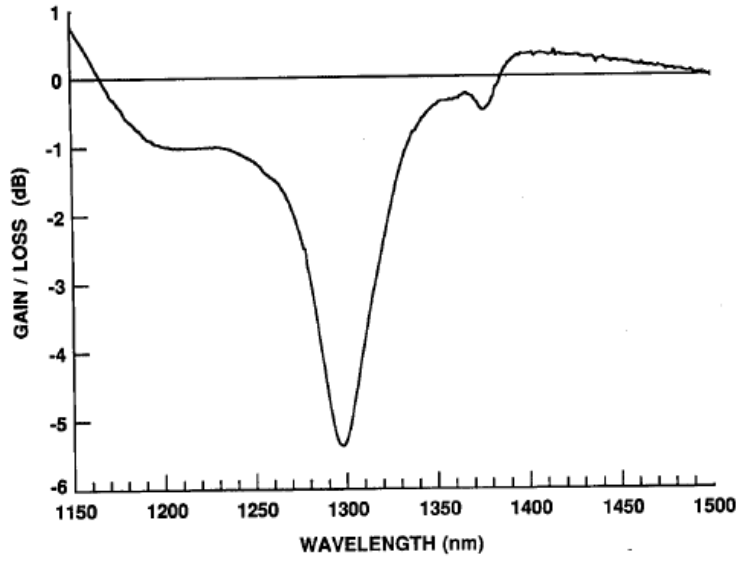

Figure 1: The gain/loss spectrum for Nd doped in a Ge-silica fiber [Miniscalco, 2001].

The figure above was generated from a silica fiber that contained germanium as well as being doped with neodymium. There are two noticeable peaks on this graph, as well, that are at nearly the same wavelengths as the two peaks in the excited state absorption cross section measured during this study.

It appears that the ESA cross section peaks of the neodymium in the silica fiber used for this experiment have been broadened and flattened such that the excited state absorption is not as strong at 1350 nm, but extends out past 1450 nm to cancel the stimulated emission. To achieve gain in this wavelength range it may be necessary to select a host glass in which the excited state absorption peaks are more sharply defined.

References

Ainslie, James with Susan P. Craig and Steven T. Davey (1988). "The Absorption and Fluorescence Spectra of Rare Earth Ions in Silica Based Monomode Fiber." *J. of Lightwave Tech.*, **6**, 287.

Belov, A.V. with E. M. Dianov and P. N. Lebedev (1982). "OH Absorption in GeO_2-Doped Fused Silica Fibres." *Electronics Letters*, **18**, 836.

Bragdon, Robert (1996). "Excited State Absorption Cross Sections in Thulium Doped Glass." M.S. Thesis, Worcester Polytechnic Institute.

Carnall, W.T. with H. Crosswhite, and H.M. Crosswhite (1977). "Energy level structure and transition probabilities of the trivalent lanthanides in LaF3", Argonne National Laboratory Report.

Carnall, W.T. with P.R. Fields and K Rajnak (1968 (1)). "Electronic Energy Levels in the Trivalent Lanthanide Aquo. Ions, I. Pr^{3+}, Nd^{3+}, Pm^{3+}, Sm^{3+}, Dy^{3+}, Ho^{3+}, and Tm^{3+}." *J. Chem. Phys.*, **49**, 4424.

Carnall, W.T. with P. R. Fields, and K. Rajnak (1968 (2)), "Spectral Intensities of the Trivalent Lanthanides and Actinides in Solution. II. Pm^{3+}, Sm^{3+}, Eu^{3+}, Gd^{3+}, Tb^{3+}, Dy^{3+}, and Ho^{3+}." *J. Chem. Phys.*, **49**, 4412.

Dragic, Peter D. and George C. Papen (1999). "Efficient Amplification Using the $^4F_{3/2} > {}^4I_{9/2}$ Transition in Nd-Doped Silica Fiber." *IEEE Phot. Tech. Letters*, V. **11**, No. 12, 1593.

Ehrmann, P.R. with K. Carlson, J.H. Campbell, C.A. Click, and R.K. Brow (2004). "Neodymium Fluorescence Quenching by Hydroxyl Groups in Phosphate Laser Glasses." *J. of Non-Crystalline Solids*, **349**, 105-114.

Gschneider, K.A. and Eyring, L (1998). Handbook on the Physics and Chemistry of Rare Earths. Volume **25**, Elsevier Science.

Martin, Rodica M (2006). "Reciprocity between Emission and Absorption for Rare Earth Ions in Glass." Ph.D. Thesis, Worcester Polytechnic Institute.

McCumber, D.E (1964). "Einstein Relations Connecting Broadband Emission and Absorption Spectra." *Phys. Rev.*, **136**, A954.

Miniscalco, William (2001). "Optical and Electronic Properties of Rare Earth Ions in Glasses." In Rare-Earth-Doped Fiber Lasers and Amplifiers, 2nd ed. Marcel Dekker.

Miniscalco, William (1991). "Erbium-Doped Glasses for Fiber Amplifiers at 1500 nm." *J. of Lightwave Tech.*, **9**, 234.

Ning, Da with Yang Iv-yun, Peng Ming-ying, Zhou Qing-ling, Chen Dan-ping, Tomoko Akai, and Kohei Kadono (2005). "Preparation and Spectroscopic Properties of Er^{3+}-Doped High Silica Glass by Sintering Nanoporous Glass." *Materials Letters*, **60**, 1987.

Quimby, Richard S (2006). Photonics and Lasers, An Introduction. John Wiley and Sons.

Quimby, Richard S (1991). "Active Phenomena in Doped Halide Glasses." In Fluoride Glass Fiber Optics, ed. By I.D. Aggarwal and G. Lu. Academic Press, p. 351.

Schubert, Fred (1993). "Light Emitting Diodes." Cambridge Univ. Press. Obtained from http://www.ecse.rpi.edu/~schubert/Light-Emitting-Diodes-dot-org/chap18/chap18.htm on July 17, 2008.

Stokowski, S.E. with R.A. Saroyan and M.J. Weber (1981). "Nd-Doped Laser Glass Spectroscopic and Physical Properties." Lawrence Livermore National Laboratory report. Livermore, CA.

Appendices

Appendix A: Equations and Constants

This appendix has been provided for the convenience of the reader when referring to equations within the text.

Equations in order of appearance:

The energy of a photon is a function of wavelength, ν, or wavelength, λ. Other factors include Planck's constant, *h*, and the speed of light, *c*:

$$E_\gamma = h\upsilon = \frac{hc}{\lambda} \tag{2.1-1}$$

The total number density per unit volume, *N*, of either erbium or neodymium is approximated as the sum of the ground state population density, N_1, and the excited state population density, N_2.

$$N = N_1 + N_2 \tag{2.3-1}$$

In the rate equation for the excited state in either erbium or neodymium, shown below, the W terms are rates and τ_2 is the lifetime of the excited state. The subscripts *p*, *gsa*, and *se* stand for pump, ground state absorption, and stimulated emission respectively.

$$\frac{dN_2}{dt} = N_1\left(W_p + W_{gsa}\right) - N_2\left(\frac{1}{\tau_2} + W_{se}\right) \tag{2.3-3}$$

The above equation was simplified assuming that a small probe signal had very little effect on the population density compared to a strong pump beam.

$$\frac{dN_2}{dt} = N_1 W_p - N_2\frac{1}{\tau_2} \tag{2.3-4}$$

The steady state excited population density as a function of pump rate, excited lifetime, and total population number density.

$$N_2 = N\frac{W_p\tau_2}{W_p\tau_2 + 1} \tag{2.3-6}$$

The pump rate used in the above equations as a function of pump intensity, I_p, ground state absorption cross section (at the pump wavelength), σ_{gsa}, Planck's constant, and the pump frequency, ν_p.

$$W_p = \frac{\sigma_{gsa} I_p}{h\upsilon_p} \tag{2.3-7}$$

Beer's Law relates the intensity at a point a distance z into a sample, $I(z)$ to the incident intensity, I_o, a reflection and scattering term, R, the absorption coefficient, α, and the path length z.

$$I(z) = I_0 \, \mathrm{Re}^{-\alpha z} \tag{2.4-3}$$

The ground state absorption cross section can be determined from the population number density, the length of the sample, L, the reflection term, as well as the final and incident intensities of a signal passing through the sample.

$$\sigma_{gsa} = \frac{1}{NL} \ln\left(\frac{RI_0}{I_f}\right) = \frac{1}{NL}\left[\ln\left(\frac{I_0}{I_f}\right) + \ln(R)\right] \tag{2.4-5}$$

The gain coefficient, is equal to the stimulated emission cross section multiplied by the excited state population density. The absorption coefficient is equivalent to the sum of the excited population times the excited state absorption cross section and the ground state population times the ground state absorption cross section.

$$\begin{aligned} \gamma &= N_2 \sigma_{se} \\ \alpha &= N_2 \sigma_{esa} + N_1 \sigma_{gsa} \end{aligned} \tag{2.5-3}$$

The average excited state population density, $\overline{N}_2$, is equivalent to the inverse of the fiber length multiplied by the integral of the excited state population number density as a function of position over the length of the fiber.

$$\overline{N}_2 = \frac{1}{L}\int_0^L N_2(z)dz \tag{2.5-6}$$

The natural log of the transmitted intensity through the pumped fiber, I_p, divided by the intensity transmitted though the un-pumped fiber, I_u, is equal to the product of the average excited state number density and the length of the fiber, multiplied by the GSA cross section plus the SE cross section minus the ESA cross section.

$$\ln\left(\frac{I^p}{I^u}\right) = \left(\sigma_{gsa} + \sigma_{se} - \sigma_{esa}\right)\overline{N}_2 L \tag{2.5-9}$$

The McCumber relation links the stimulated emission cross section with the probability a photon will be emitted in one second per unit frequency interval per unit solid angle, f_λ. Other terms include the Einstein A coefficient, A_2, solid angle, Ω, angular frequency, ω, and the index of refraction in the medium, $n(\lambda)$.

$$f_\lambda(\omega) = \sigma_{se}\left[\frac{n(\lambda)\omega}{2\pi c}\right]^2 \tag{2.6-1}$$

$$A_2 = \sum_\lambda \int_{4\pi} d\Omega_{k\lambda} \int \frac{d\omega}{2\pi} f_\lambda(\omega)_2 \tag{2.6-2}$$

The stimulated emission cross section is equal to the fluorescence power as function of wavelength, $\Delta P(\lambda)$, multiplied by the wavelength to the fifth power, divided by the speed of light squared, the index of refraction squared, Planck's constant, the solid angle being observed, multiplied by the wavelength interval (or resolution).

$$\sigma_{se} = \frac{\Delta P(\lambda)\lambda^5}{c^2 n^2(\lambda) h\Omega\Delta\lambda} \tag{2.6-6}$$

$$\sigma_{se} \propto \frac{\Delta P\lambda^5}{n^2} \tag{2.6-7}$$

The total oscillator strength of a transition, f, is equal to the sum of the electric dipole oscillator strength, f_{ed}, and the magnetic dipole oscillator strength, f_{md}.

$$f = f_{ed} + f_{md} \tag{2.7-1}$$

The emission and absorption oscillator strengths between the same two levels are related by the ratio of the degeneracy of the lower level, g_1, to the degeneracy of the upper level, g_2.

$$f_{emit} = \frac{g_1}{g_2} f_{abs} \tag{2.7-2}$$

In the equation below for the electric dipole oscillator strength between two energy states, m is the mass of an electron, λ is the wavelength of a photon with energy equal to the difference between the two levels, and J_i is the J quantum number of the initial state. The quantity $\left\langle a \middle\| U^t \middle\| b \right\rangle$ is the doubly reduced matrix element of the tensor operator U^t between the two levels, a and b, and Ω_t are the Judd-Ofelt parameters.

$$f_{ed} = \frac{8\pi^2 mc\chi_{ed}}{3h\lambda(2J_i+1)n^2} \sum_{t=2,4,6} \Omega_t \left| \left\langle a \middle\| U^t \middle\| b \right\rangle \right|^2 \tag{2.7-3}$$

$$\text{Where} \quad \chi_{ed} = \frac{n(n^2+2)^2}{9}$$

The magnetic dipole oscillator strength is calculated using many of the same parameters as the above equation, however, L and S stand for the angular momentum and spin operators, respectively.

$$f_{md} = \frac{hc\chi_{md}}{6\lambda(2J_i+1)n^2mc^2} \left| \left\langle a \middle\| L + 2S \middle\| b \right\rangle \right|^2 \tag{2.7-4}$$

$$\text{Where} \quad \chi_{ed} = \frac{n(n^2+2)^2}{9}$$

The total integral of a transition cross section is related to the oscillator strength of that transition. ε_0 is the permittivity of free space and e is the electron charge.

$$\int \sigma(\lambda) \frac{c}{\lambda^2} d\lambda = \frac{e^2}{4mc\varepsilon_0} \left(f_{ed} + f_{md} \right) \tag{2.7-6}$$

The Planck distribution describes the spectral energy density, per unit wavelength interval. In this equation, T is the temperature in Kelvin and k_B is Boltzmann's constant.

$$\rho(\lambda)d\lambda = \frac{8\pi h}{\lambda^3}\frac{1}{\exp\left(\frac{hc}{k_B T\lambda}\right)-1}\frac{c}{\lambda^2}d\lambda = \frac{8\pi hc}{\lambda^5}\frac{1}{\exp\left(\frac{hc}{k_B T\lambda}\right)-1}d\lambda \qquad (2.9\text{-}2)$$

The peak wavelength of a blackbody emission spectrum, λ_{max}, is dependent on the temperature of the emitter.

$$\lambda_{\max} T = 2.8977685\times 10^6\, nm\cdot K \qquad (2.9\text{-}3)$$

The transmission, T, and reflection, R, of a neutral density filter are determined by its optical density, OD.

$$\begin{aligned} T &= 10^{-OD} \\ R &= 1-10^{-OD} \end{aligned} \qquad (3.2\text{-}1)$$

Constants, in order of appearance:

Planck's Constant	$h = 6.6261x10^{-34}\left[\frac{m^2 kg}{s}\right]$
Speed of light in vacuum	$c = 2.998x10^{8}\left[\frac{m}{s}\right]$
Refractive index of silica glass	$n = 1.462$
Mass of electron	$m = 9.1094x10^{-31}[kg]$
Permittivity of Free Space	$\varepsilon_0 = 8.8542x10^{-12}\left[\frac{C^2 s^2}{m^3 kg}\right]$
Boltzmann's Constant	$k_B = 1.3807x10^{-23}\left[\frac{m^2 kg}{s^2 K}\right]$

Appendix B: Optical Spectrum Analyzer Measurements

The Optical Spectrum Analyzer (OSA) was used at the beginning of the data collection process in order to become more familiar with the fiber coupling and cleaving procedures, as well as to determine its feasibility as the data collection apparatus for this experiment. On the maximum sensitivity, the signal strength of the tungsten bulb light coupled directly into a clear multimode fiber was small and the S-N-R was poor. The OSA data collection system, is calibrated for its wavelength range of 600 to 1750 nm, although it is most effective for wavelengths longer than 1300 nm. The tungsten bulb spectrum was measured over this range on the OSA to determine the peak wavelength of the emission spectrum.

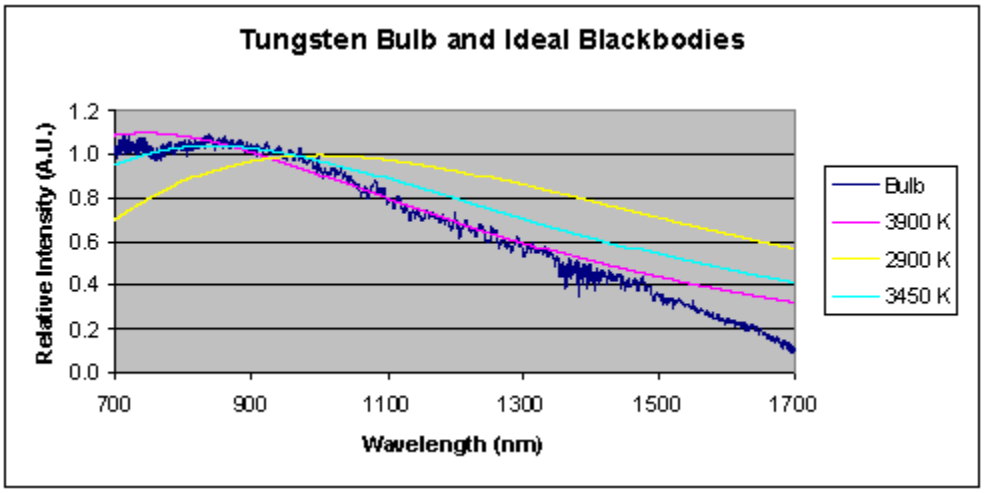

Figure 44: The tungsten bulb spectrum measured on the optical spectrum analyzer along with three theoretical blackbody curves at different temperatures.

The peak emission wavelength of the measured tungsten bulb curve was determined to be 840 nm. Using Wein's Displacement law, the effective temperature of the tungsten bulb was calculated to be 3450 Kelvin. The blackbody spectrum for 3450 K fits at the peak, but does not fit at wavelengths longer than 900 nm. The middle portion of the measured curve is best fit by a temperature of 3900 K. However, when the bulb spectrum was studied by Martin [2006], a temperature of 2900 K was used. This result is consistent with the temperature range expected by the manufacturer. This casts doubt upon the calibration of the OSA apparatus.